AD-782 350

ADVANCED CONCEPTS IN STRUCTURAL MATERIALS AND TESTING. PART II. DEVELOPMENT OF A MODULATED-MICRO-STRUCTURE HEAT TREATABLE STEEL

Peter G. Winchell, et al

Purdue University

Prepared for:

Advanced Research Projects Agency

15 July 1974

UNCLASSIFIED

Security Classification

AD-782350

DOCUMENT CONTROL DATA - R & D

(Security classification of title, body of abstract and indexing annotation must be entered when the overall report is classified)

1. ORIGINATING ACTIVITY (Corporate author)	2a. REPORT SECURITY CLASSIFICATION
Purdue Research Foundation - School of Electrical Engineering	2b. GROUP

3. REPORT TITLE

Advanced Concepts in Structural Materials and Testing
PART II. Development of a Modulated-Microstructure Heat Treatable Steel

4. DESCRIPTIVE NOTES (Type of report and inclusive dates)

Annual Technical Report 6/1/73 - 5/31/74

5. AUTHOR(S) (First name, middle initial, last name)

Peter G. Winchell
Y. C. Chen

6. REPORT DATE	7a. TOTAL NO. OF PAGES	7b. NO. OF REFS
July 15, 1974	66	8

8a. CONTRACT OR GRANT NO	9a. ORIGINATOR'S REPORT NUMBER(S)
DAHC15-73-G12	
b. PROJECT NO. ARPA Order No. 2338 Code No. 3D10	
c.	9b. OTHER REPORT NO(S) (Any other numbers that may be assigned this report)
d.	

10. DISTRIBUTION STATEMENT

Distribution of this document is unlimited.

11. SUPPLEMENTARY NOTES	12. SPONSORING MILITARY ACTIVITY
	Defense Advanced Research Projects Agency 1400 Wilson Blvd. Arlington, VA 22209

13. ABSTRACT

The work performed under this program can be subdivided into two areas. The first deals with the application of random signal correlation techniques to ultrasonic flaw detection in solids and the second deals with the development of modulated microstructure heat treatable steel.

The objective of the modulated microstructure work is to develop an alloy complex which combines high strength and significant fracture toughness. The basic concept is to alternate layers of high-strength martensite with tough and softer austenite in a complex which can be hardened to strength of 400 Ksi (2.8 GN/m^2) and softened for fabrication by conventional heat treatment.

Since the beginning of work on June 1, 1973, a preliminary experimental program has been completed and a tentative theoretical strategy has been developed. In the experimental program a technique of fabricating the alloy complex has been developed and complexes comprised of a trial pair of alloy layers have been produced, tested, and evaluated. On the basis of the resulting mechanical properties and the observed fracture path, a tentative rational method of optimizing the properties of the alloy complex has been formulated.

i

DD FORM 1 NOV 1473 (PAGE 1) PLATE NO. 21856

S/N 0102-014-6600

UNCLASSIFIED

Security Classification

14 KEY WORDS	LINK A		LINK B		LINK C	
	ROLE	WT	ROLE	WT	ROLE	WT
flaw detection modulated microstructure steel						

Annual Technical Report
for the Period 6/1/73 - 5/31/74

Advanced Concepts in Structural Materials and Testing

PART II

Development of a Modulated-Microstructure Heat Treatable Steel

Grant Number DAHC15-73-G12

Program Code No. 3D10

Grantee: Purdue Research Foundation

Project Director: R. J. Schwartz (317) 749-2467

Principal Investigators: P. G. Winchell (317) 494-8629

Y. C. Chen (317) 494-4167

Effective Date of Grant: 6/1/73

Grant Expiration Date: 5/31/74

Amount of Grant: $77,942.00

Sponsored by
Advanced Research Projects Agency
ARPA Order No. 2338

TABLE OF CONTENTS

FIGURE CAPTIONS

Figure 1. Summary of Mechanical Properties of Alloy Steel and the 1970 Technological Limit, After Lange (1971). The target strength of 400 Ksi (2.8 GN/m^2) and toughness of 150 $Ksi\sqrt{in.}$ (165 $MN/m^2\sqrt{m}$) are well above this limit.

Figure 2. Tensile Specimen Specification. The nominal thickness of specimen is .080" (2.0 mm).

Figure 3. Specimen for Interfacial Bonding Energy Measurement.

Figure 4. Pin-Loaded Grip for Tensile Test.

Figure 5. Plot of Interfacial Bonding Energy (γ) versus Oxidation Time.

Figure 6. The Stress-Strain Curves for Solid 01 Steel and Solid Purdue Soft Alloy S2.

Figure 7. The Stress-Strain Curves for Specimens with No Oxidation Treatment Prior to Hot-Roll Welding.

Figure 8. The Stress-Strain Curves for Specimens with 1 hr. Oxidation at 600°C.

Figure 9. The Stress-Strain Curves for Specimens with 2 hrs. Oxidation at 600°C.

Figure 10. The Stress-Strain Curves for Specimens with 3 hrs. Oxidation at 600°C.

Figure 11. The Tensile Stress,.1% Yield Stress and Plastic Strain As a Function of Oxidation Time for Specimens with fs = .50.

Figure 12. The Percent Reduction in Area As a Function of Oxidation Time for Specimens with fs = .50.

Figure 13. The Stress-Strain Curves for Specimens with fs = 0, .25, .50, .75, and 1.00. All specimens were oxidized at 600°C for 2 hrs. prior to hot-roll welding.

Figure 14. The Tensile Stress and .1% Yield Stress As a Function of Fraction of Soft Layer for the Same Specimens as in Figure 13. Arrows at the upper left corner of the figure represent the upper and lower bounds of 01 steel strength converted from microhardness data.

Figure 15. The Plastic Strain As a Function of Fraction of Soft layer for the Same Specimens as in Figure 13.

Figure 16. The Percent Reduction in Area As a Function of Fraction of Soft Layer for the same Specimens as in Figure 13.

Figure 17. The Microstructure of a Specimen Oxidized at 600°C for 1/2 hr. Prior to Hot-Roll Welding. The dark particles in the central portion of the micrograph are oxide particles. Magnification 3000x.

Figure 18. The Microstructure of Specimen D 121. The dark areas represent the hard layer (O1 Steel) consisting of fine martensite with a small amount of retained austenite. The light areas are the soft layer (Purdue S2 alloy) in which the martensite appears to have larger plate size. Magnification 80x.

Figure 19. The Microhardness As a Function of Distance in Modulation Direction for Specimen D 121.

Figure 20. The Microhardness of the Central Hard Layer As a Function of Distance Along the Tensile Axis for Specimen D 121.

Figure 21. A Schematic Fractograph for Specimen D 112. The crack originated from H_2, S_3, and H_3 area. The shear fracture modes dominated except in H_2, H_3, and H_4 where brittle fracture occurred. No debonding or necking was observed.

Figure 21A. A Micrograph Showing the Fracture Surface of Specimen D 112. Magnification 100x.

Figure 22. A Schematic Fractograph for Specimen D 221. Again shear fracture modes dominated except in H_3 and H_4 some small amount of debonding was observed.

Figure 23. A Schematic Fractograph for Specimen D 312. Except flat brittle fracture in H_2 and H_3, the shear fracture modes were observed. Some neckings at edge and more partial debonding were observed. Crack originated from either H_1 or H_2.

Figure 24. A Schematic Fractograph for Specimen D 411. There are more typical cone and cup tensile fracture characteristics at edges, more debonding. Shear fracture modes were observed except H_3 and H_4. The crack originated from the central portion of H_3.

Figure 24A. A Micrograph Showing the Fracture Surface of Specimen D 411. Magnification 100x.

Figure 25. A Schematic Fractograph for Specimen D 304 (fs = 0). Crack originated from the interface between H_5 and H_6. Brittle fracture occured in the upper half of the specimen and shear dimple type in the lower half. The interfaces were indistinguishable.

Figure 25A. A Micrograph Showing the Fracture Surface of Specimen D 304. Magnification 100x.

Figure 26. A Schematic Fractograph for Specimen D 332 (fs = .25). Brittle fracture occured in hard layers and shear fracture occured in soft layers. Crack originated from H_5 propagating to the left of the specimen. Multiple crack nucleation sites were observed in hard layers.

Figure 26A. A Micrograph Showing the Fracture Surface of Specimen D 332. Magnification 100x.

I. Introduction.

The objective of the work is to develop an alloy complex of modulated-microstructure steel (MMS) which combines high strength and significant fracture toughness. The basic concept is to alternate layers of high-strength martensite with tough and softer austenite in a complex which can be hardened to strength of 400 ksi (2.8 GN/m^2) and softened for fabrication by conventional heat treatment.

This development can best be viewed against the presently available mechanical properties of alloy steels. These properties are summarized by Lange [1] as presented in Figure 1. His estimate of the high strength technological limit of fracture toughness is substantially less than 100 $ksi\sqrt{in.}$ (.11 $GN/m^2\sqrt{m}$) at stress levels in excess of 300 ksi (2.1 GN/m^2). The proposed alloy should obtain strength of 400 ksi (2.8 GN/m^2) and has a target fracture toughness of 150 $ksi\sqrt{in.}$ (.16 $GN/m^2\sqrt{m}$). This represents a technologically attractive design objective and work is proceeding toward it.

In the first half of the year (Phase I), an alloy complex was developed and complexes comprised of a trial pair of alloy layers were produced, tested, and evaluated under Phase I of the project. On the basis of the resulting mechanical properties and the observed fracture path, a tentative rational method of optimizing the properties of the alloy complex has been formulated.

In the second half of the year, the rational method was applied to a new alloy complex as Phase II of the project. The new alloy complex contains partially debonded layers so that deformation of neighboring layers is partially decoupled. Efforts were focused on the effect of retained oxides in interfaces and the effect of the soft layer fraction (fs) on the tensile properties of the alloy complex.

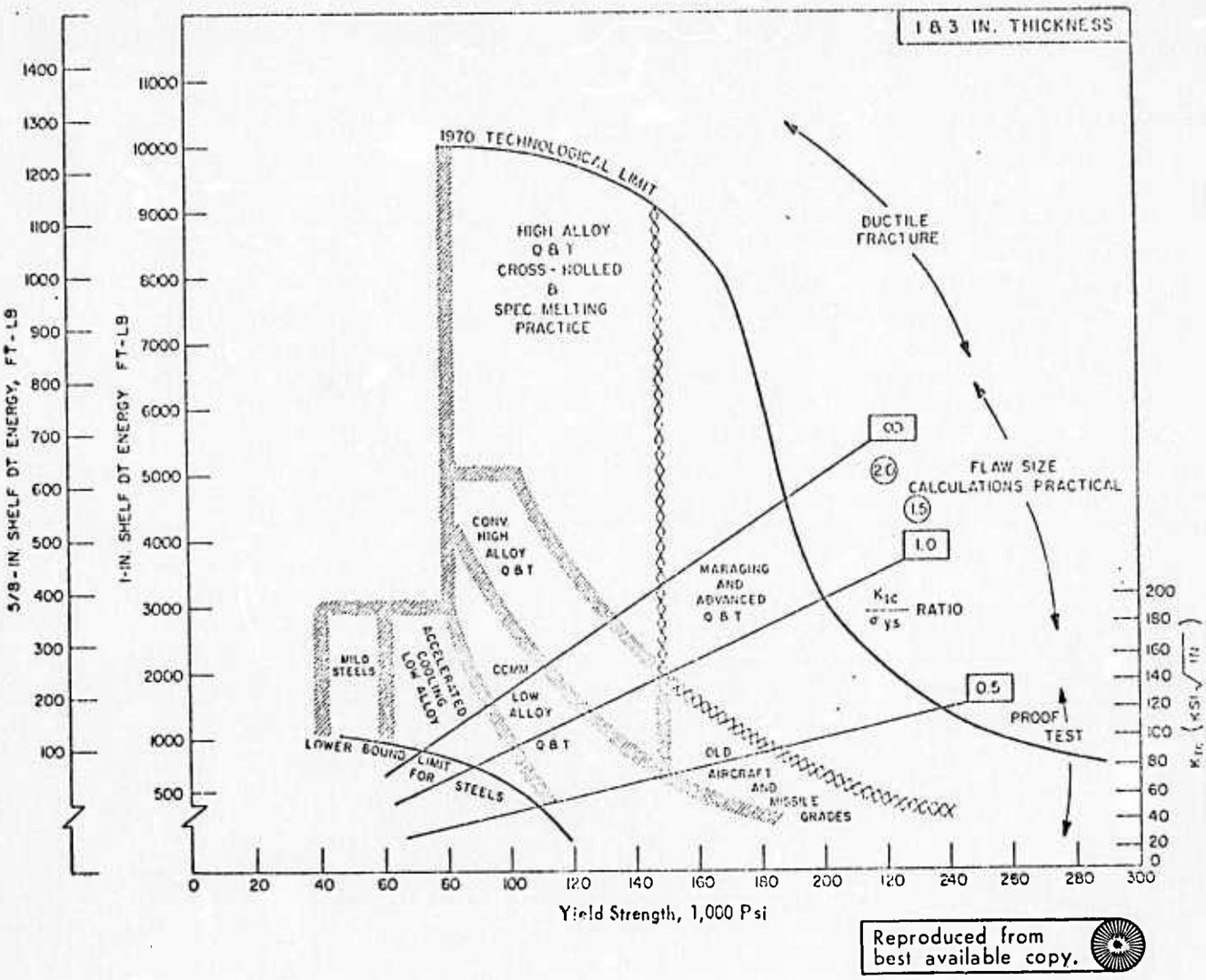

Figure 1. Summary of Mechanical Properties of Alloy Steel and the 1970 Technological Limit, After Lange (1971). The target strength of 400 Ksi (2.8 GN/m^2) and toughness of 150 Ksi$\sqrt{in.}$ (165 $MN/m^2\sqrt{m}$) are well above this limit.

II. Experiments.

2.1. Selection of Alloy System.

The hard layer for Phase II system was again AISI type O1 tool steel because of its low cost and commercial availability. To match O1 steel, a Purdue soft layer alloy (S2) was designed based on the following criteria: (a) reasonably high ductility, (b) strength of about 150 ksi (1.0 GN/m^2), (c) carbon potential equal to that of the hard layer, (d) heat treatment compatible with that of the hard layer. In order to meet these criteria an iron-nickel-cobalt-carbon alloy was selected with Ms=0°C and cobalt level sufficiently high to suppress deformation twinning in the martensite. The composition shown for S2 in Table I meets these requirements. It is compatible in carbon potential and heat treatment with O1 steel and it may be subzero quenched to produce martensite at any stage in the treatment. Such subzero quenching has little effect on the O1 steel. The retained austenite can transform during deformation and fracture[2,3] to increase fracture toughness.

The compositions for both hard and soft alloy steels are shown in Table I.

TABLE I

Composition of Trial System.

(wt.%)

Material	Elements C	Mn	Cr	W	V	Ni	Co	Fe
AISI type O1*	.90%	1.20%	.50%	.50%	.20%	0	0	Balance
S2**	.38%					25.2%	6%	Balance

* Compositions are nominal.

** Compositions are as-charged values. Actual carbon content may be .02% lower.

2.2. Experimental Program.

2.2.1 Preliminary Experiments.

As stated in the previous renewal proposal[4], the bonding between the hard and soft layers appears to be of great importance. A significant result of the Phase I experimental work is that deformation of the soft layer is prevented by fully bonded adjacent hard layers. In Phase II, the efforts were focused on the development and evaluation of partially debonded interfaces on the tensile properties of the Phase II alloy complex.

Two techniques of partial debonding were studied, oxidation of one of the interfacing surfaces and sprinkling aluminum oxide particles on the interfacing surfaces prior to hot-roll welding. These pretreatments result in small oxide particles being retained in the interface. Microscopic examination of the interfaces for products of both techniques showed that the resulting interface by sprinkling of Al_2O_3 particles on the interfacing surfaces were inferior to that of oxidation method. If the Al_2O_3 particles were large, they tended to penetrate the layers and disturb layer morphology. If the Al_2O_3 particles were small, they were difficult to distribute uniformly in the interfaces. Another disadvantage of using Al_2O_3 is that some of the particles tended to break up during rolling, and the resultant oxides in interfaces were not uniform in size. These problems did not exist for oxidation method. Moreover, tearing apart of layers at interfaces produced with the oxidation method seemed to give more uniform separation than was the case for interfaces produced with Al_2O_3 addition. The oxidation method was therefore chosen for further study.

The extent of oxidation obtained at certain temperature and time was investigated. Several trial sets of samples were oxidized at different temperatures for different times. The samples were weighed and the amount of oxide calculated. The desirable oxidation temperature for O1 steel was chosen to be 600°C. In addition to the unoxidized case, the range of oxidation times was then selected from 5 minutes to 3 hours and the resulting interfaces varied from well bonded to poorly bonded.

The interfacial bonding is to be characterized by measurement of energy required to propagate a crack in the interface[5] and will be discussed in detail in a later section.

2.2.2 O1-Purdue S2 Tests.

After the preliminary experiments, a systematic program was implemented to investigate the effect of interfacial bonding on the tensile properties of the alloy complex. Oxidation treatment of layers at 600°C for 0 hour, 1 hour, 2 hours, and 3 hours were selected. For each treatment four samples were produced at the 0.5 fraction soft layer (f_s = .5). Another series of samples received the 2 hours oxidation treatment while fraction of soft layer varied from 0 to 1.0.

For mechanical testing a standard sample was required. Each sample contained eleven layers in total, five hard layers and six soft layers. The outer layers were soft ones which might reduce the possibility of specimen cracking originating at exterior surface flaws. For convenience in mechanical testing as well as to keep materials costs low, the specimen thickness was kept around .080"(2mm),i.e., a wavelength of about .015"(.4 mm). All the specimen were to be heat treated and tested at the same condition which will be described in a latter section. Table II gives a summary of all specimens, their oxidation

TABLE II

Summary of Specimen Identification, Treatment,
and Volumetric Fraction of Soft Layer.

Fraction Soft Layer fs / OXIDATION TREATMENT	0.0		0.25	0.5	0.75	1.00	
	Solid	Laminated	Laminated	Laminated	Laminated	Laminated	Solid
None	D 021			D 111			DP 1
	D 022			D 112			DP 2
	D 023			D 121			DP 3
	D 024			D 122			
1 hr at 600°C				D 211			
				D 212			
				D 221			
				D 222			
2 hrs at 600°C		D 301	D 331	D 311	D 351	D3P1	
		D 302	D 332	D 312	D 352	D3P2	
		D 303	D 333	D 321	D 353	D3P3	
		D 304	D 334	D 322	D 354	D3P4	
3 hrs at 600°C				D 411			
				D 412			
				D 421			
				D 422			

treatment prior to hot-roll welding, and the volumetric fraction of soft layer for this study.

2.3 Manufacturing Techniques.

2.3.1 Soft Layer Alloy Fabrication.

The Purdue soft layer alloy S2 was manufactured at the crystal growing facility at Purdue University[6]. The metallic elemental charge of the right composition for S2 alloy was placed in a 99.8% alumina crucible and induction heated in vacuum. After the charge was melted down, a partial pressure of CO was admitted to the system and the carbon was added into the melt. The introduction of CO gas was to prevent loss of carbon in reacting with the crucible. When the temperature of the melt was stablized. The casting followed. The RF power was turned off. The system was pumped out and the fused silica draw tube was lowered into the melt. The system was pressurized with Ar gas while the draw tube was being pumped on to remove any gas that might be generated by the hot metal. The melt was sucked up in the draw tube until it contacted a chill, made of plain carbon steel. Solidification of the alloy was complete in a very short time after the draw; thus, segregation and inhomogeneous microstructure were avoided.

The solid rod product was then cut into pieces of proper sizes and enclosed in preoxidized, sealed stainless steel tubes for hot rolling to the desired thickness.

2.3.2 Manufacturing of Alloy Complexes.

The techniques of manufacturing the alloy complex had been developed in Phase I. The procedures were described in the previous report. (For detail, see §2.3.1 in the First Semiannual Report[7]).

Briefly, sheets of O1 steel and S2 alloy were cut to the proper dimension and cleaned in an ultrasonic cleaner. The stack of alternating layers of O1 steel and S2 alloy was enclosed in a stainless steel container which prevented oxidation of the sample during hot-rolling process. Preoxidation of the stainless steel container at 950°C for 15 minutes was necessary in order to avoid sticking of the stainless steel to the sample after hot-rolling.

The whole container was heated to 1150°C prior to rolling. Typical heating time was about 10 minutes prior to rolling and typical reduction per pass was 0.1". After rolled to the desired thickness, the stainless steel container was removed by sawing off the edges and forcing a chisel between the sample and the stainless steel. Every as-rolled sample was annealed at 675°C for 1 hour and then cut to pieces 4" long and 1" wide for machining to tensile specimen specification (Figure 2).

2.4. Heat Treatment.

Every tensile specimen received identical heat treatments as follows:

(a) enclosed in a container, heated at 700°C for 20 minutes in a lead pot.
(b) quenched in oil, then in liquid nitrogen for 30 minutes.
(c) clamped flat with stainless steel plates, enclosed in a container, heated to 830°C for 1 hour.
(d) quenched in oil, then in liquid nitrogen for 30 minutes.
(e) tempered at 200°C for 1 hour.

The reason for the first thermal cycle ((a) & (b)) used in the above procedure was to refine the martensite plate size[8] in the soft layer.

2.5. Interfacial Bonding Measurement.

There are several methods to characterize interfacial bonding. The method chosen here was similar to the one Gilman[5] used to measure the surface energy of various single crystals. In this method a partially split

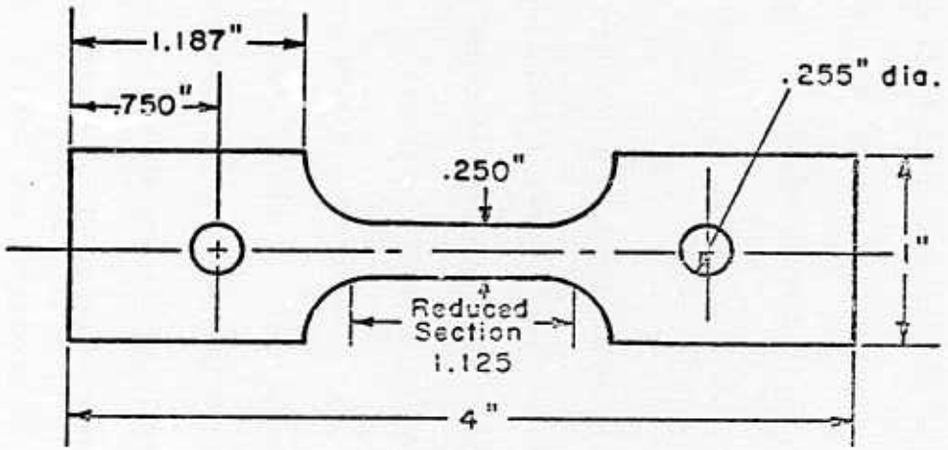

Figure 2. Tensile Specimen Specification. The nominal thickness of specimen is .080" (2.0 mm).

specimen, (Figure 3), is loaded as a double cantilever beam and the force required to propagate the crack recorded. Knowing the original crack length and the width of the sample, the interfacial bonding energy density, γ, can be calculated according to [5]:

$$\gamma = \frac{6F^2 L^2}{Ew^2 t^3} , \qquad (1)$$

where t is the half thickness, F is the force, L the crack length, w the width, and E is Young's modulus. For the case where the split is not centered, γ can be written as

$$\gamma = \frac{3F^2 L^2}{E w^2} \left(\frac{1}{t_1^3} + \frac{1}{t_2^3} \right), \qquad (2)$$

where t_1 and t_2 are thickness of the upper and the lower halves.

For the present tests, special four layer sheets comprised of alternating hard and soft layers of equal thickness were produced by the standard techniques. A four-layer sheet was prepared using each of the following oxidation treatments: no oxidation, 1/2 hr., 1 hr., 1 1/2 hrs., 2 hrs., 2 1/2 hrs., 3 hrs. at 600°C. Five specimens 1" x 13/16" x .031" were prepared from each sheet. The specimens were heat treated as prescribed in Section 2.4. A hole was cut by electro discharge machining (EDM) as indicated in Figure 3. By means of a sharp wedge forced against the specimen end, a crack was introduced in the center interface. The crack was propogated until it extended to about half the specimen length. Specimens with irregular cracks were rejected .

The specimens were then tested in an Instron machine by clamping the wires (Figure 3) in standard friction-type grips. When the crack began to increase in length, the applied force decreased suddenly because of the increased deflection of ends of the specimen. The force at which this happened was recorded as critical force for crack propagation. The crack

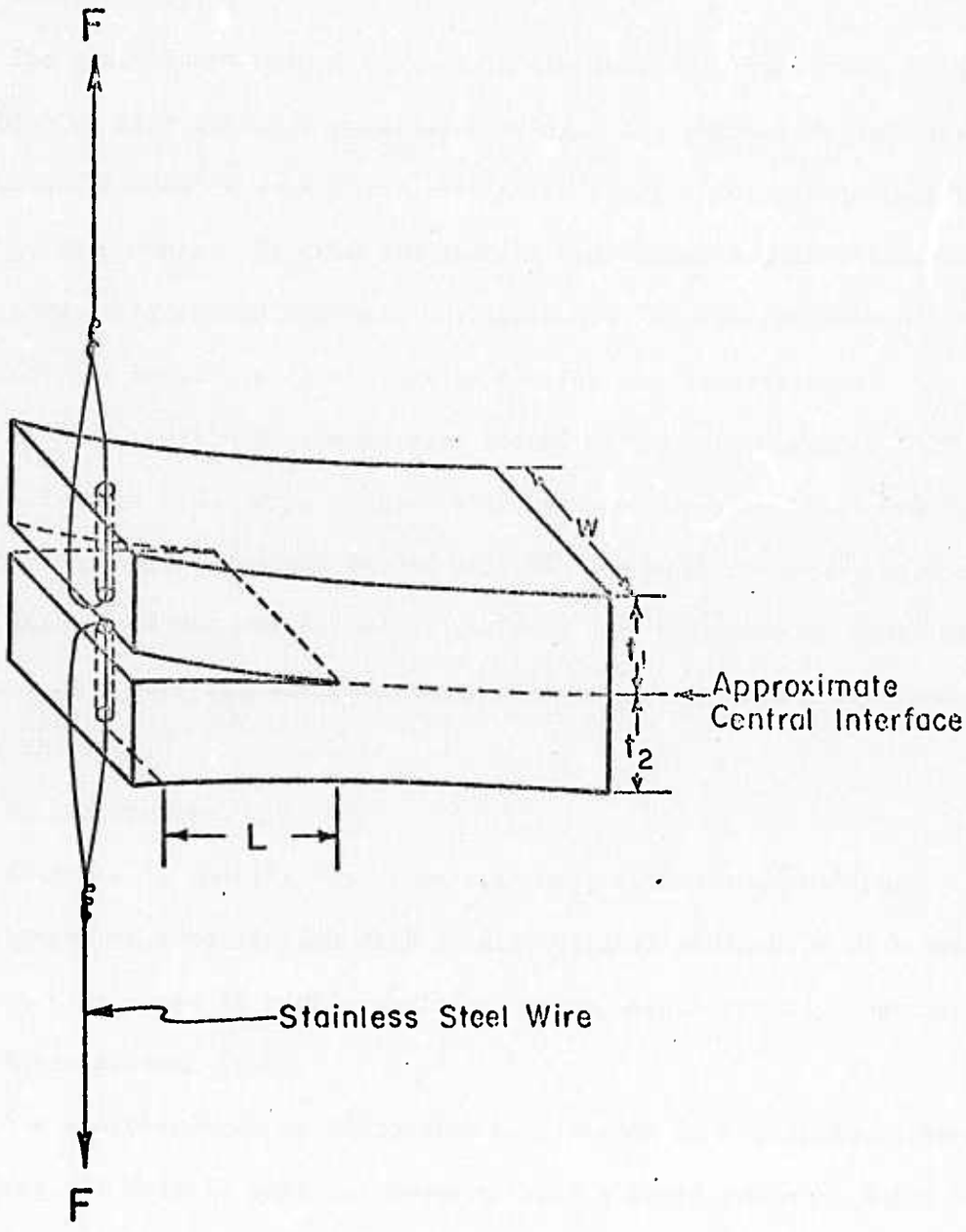

Figure 3. Specimen for Interfacial Bonding Energy Measurement.

lengths were measured microscopically. The interfacial bonding energy was calculated by means of Equation 2.

2.6. Tensile Test.

The preliminary design of tensile specimen in Phase I was found not suitable for high strength material testing. The present design (see Figure 2) utilize pin-loaded concept which eliminates the griping problem exhibited in Phase I experiments. To hold the tensile specimens, a pair of pin-loaded grips were designed and machined (Figure 4). The performance of these grips and the tensile specimen during testing was satisfactory.

All the tensile specimens were tested at room temperature (∿22°C) with an Instron Floor Type machine with maximum capacity of 10,000 lbs. A strain gauge extensometer (model G-51-16) was used to record strain. The cross head speed was maintained at .02"/min. at all times so that the strain rate was identical for all specimens. The force and strain were recorded during the test.

2.7. Microstructure.

Sections of tensile test specimens were mounted and polished. The microstructures were studied with a Leitz optical microscope or a scanning electron microscope if high magnification was needed for fine details.

2.8. Microhardness Test.

The microhardness as a function of distance in modulation direction and along the tensile axis was measured with a Knoop indentor and a 400 grams load. This measurement was used as a test of proper quenching of the tensile specimen and to obtain information on the hard and soft layer strength levels in the complex as compared to each single component.

III. Experimental Results and Discussion.

3.1. Interfacial Bonding Energy Measurement (Preliminary).

The interfacial bonding energies obtained for various oxidation

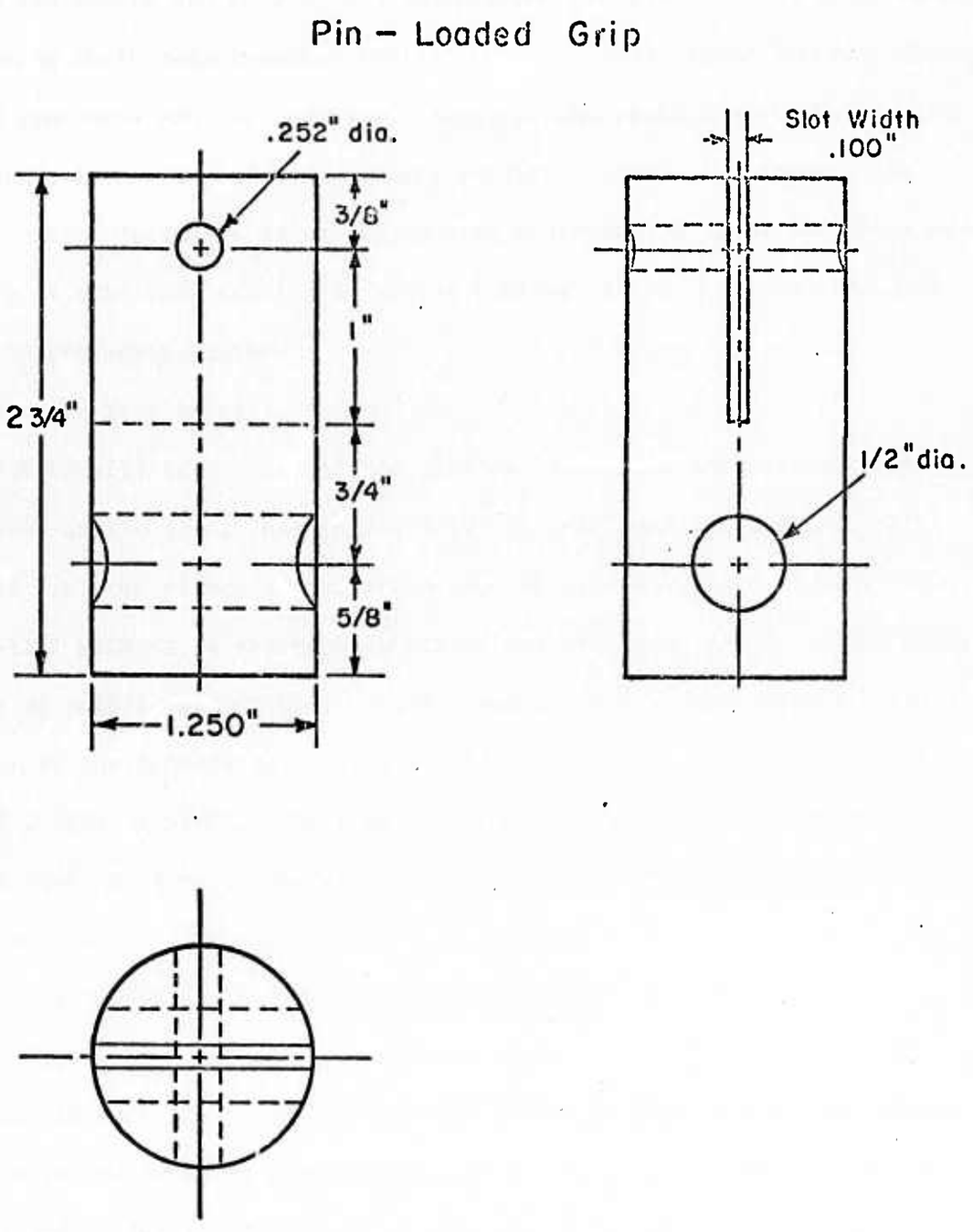

Figure 4. Pin-Loaded Grip for Tensile Test.

treatments by means of the techniques described in Section 2.5. are shown in Figure 5. These results are regarded as tentative because the specimens have so few layers and because the measurement technique was under development during their measurement. Further tests on underformed portions of tensile specimens are now underway. Even so, the preliminary data do show a reduction in bonding with increasing oxidation time. The interfacial bonding energy decreases as oxidation time increases as expected, since increasing of oxidation results in poorer bonding, therefore, requires less energy to propagate cracks.

3.2. Tensile Test Results.

The tensile test data will be divided into three subsections: (a) the stress-strain (σ-ε) curves for solid 01 steel and solid Purdue soft alloy S2; (b) the effect of oxidation time of each individual layers prior to hot-roll welding on the tensile properties of alloy complex at the fifty percent of soft layers (i.e. fs = .50); and (c) the effect of soft layer fraction on the tensile properties of alloy complex at a constant oxidation time of 2 hrs. at 600°C. The data for specimens which failed outside the reduced section were not included except for cases where ductility was very low, i.e., fs = 0 and fs = .25.

3.2.1 σ-ε Curves for Solid Single Components.

Figure 6 shows the σ-ε characteristics for solid 01 steel and solid Purdue soft alloy S2. The 01 steel after hardening and light tempering is expected to be of high strength ($\sim$ 340 Ksi or 2.3 GN/m^2) and to be brittle and Purdue soft alloy S2 is expected to be ductile and of lower strength. The measured strength for 01 was around 300 Ksi (2.1 GN/m^2), not far from the expected value, and no plastic strain was observed. The tensile strength for S2 was around 180 Ksi (1.2 GN/m^2) and the total strain was

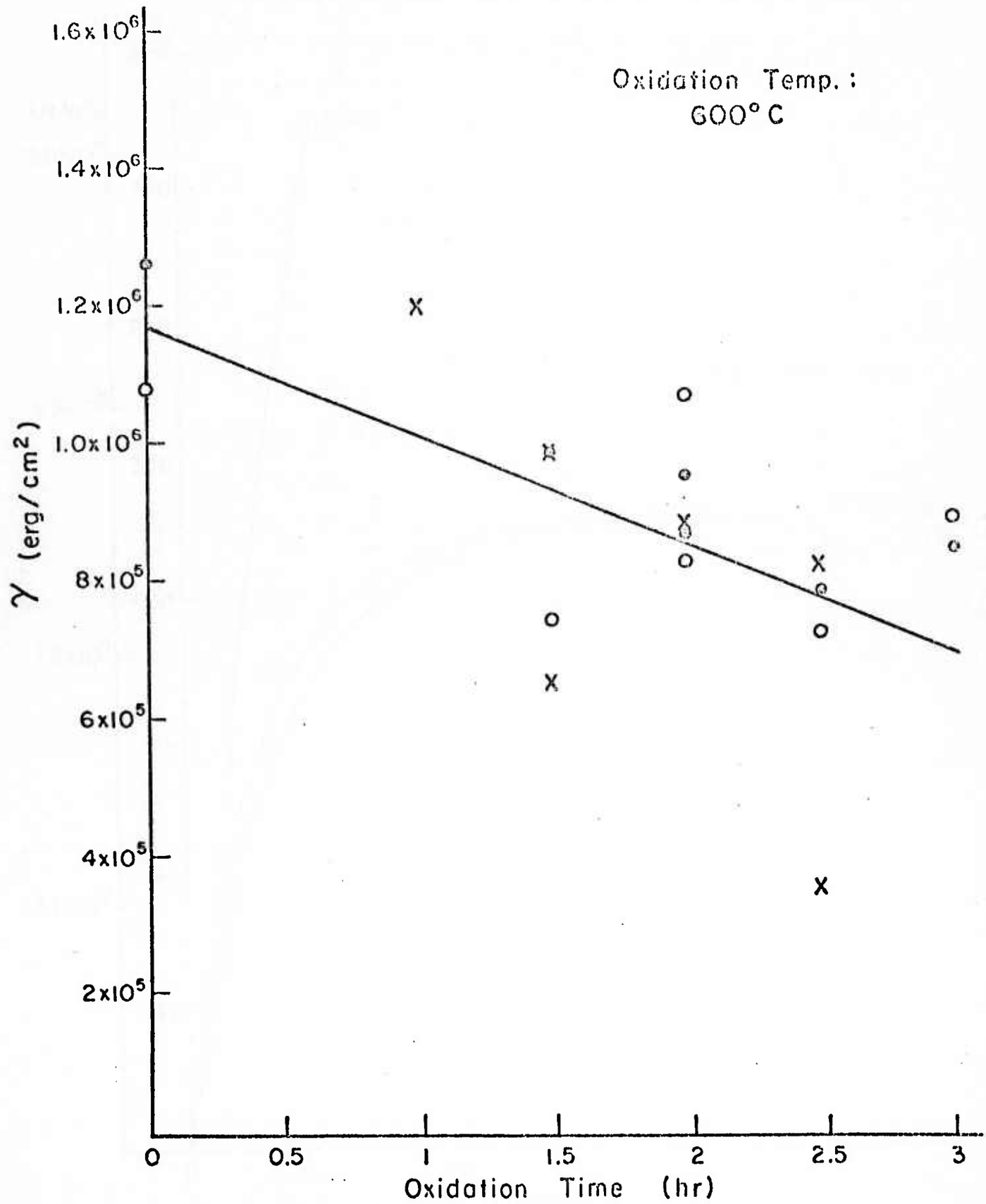

Figure 5. Plot of Interfacial Bonding Energy (γ) versus Oxidation Time.

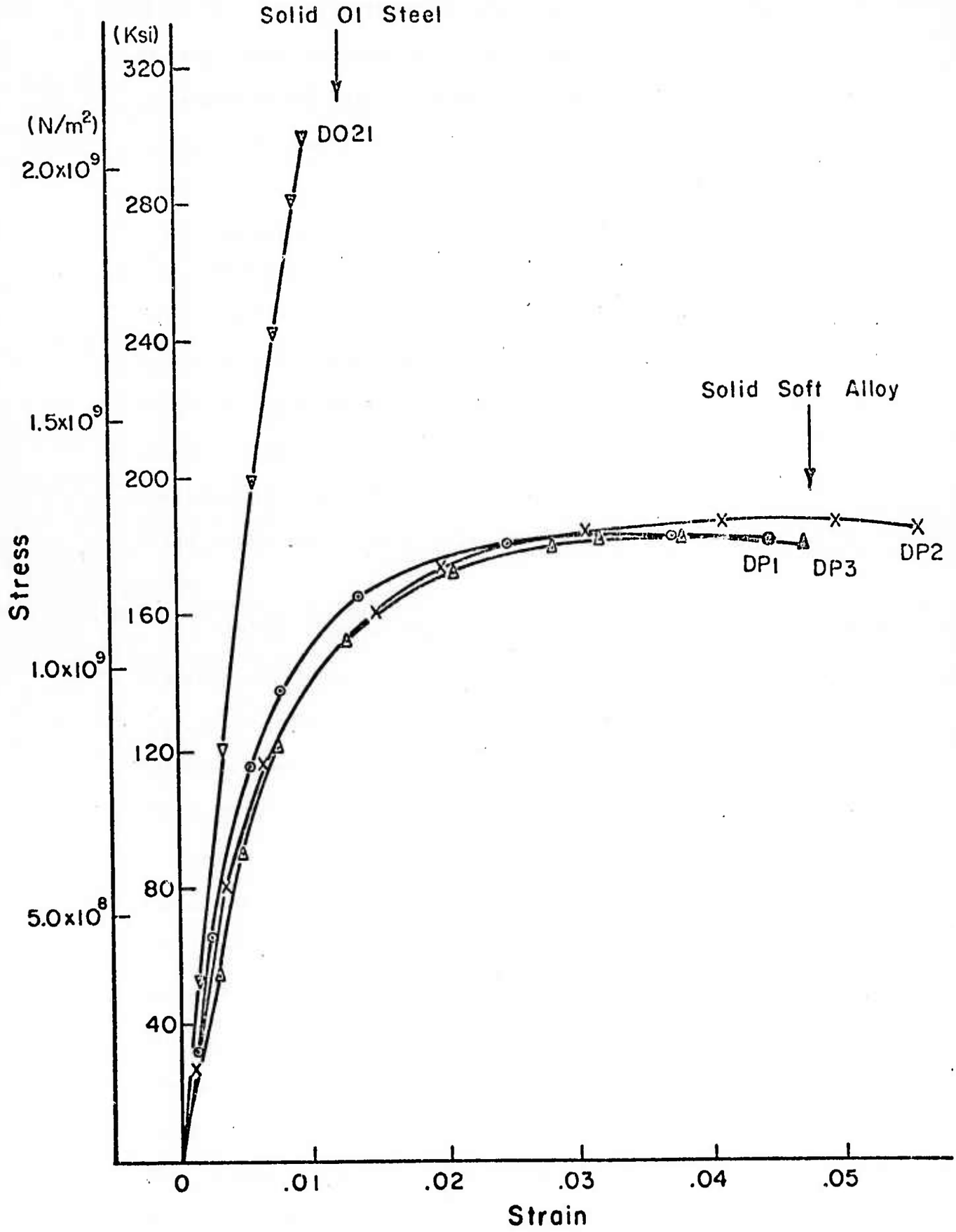

Figure 6. The Stress-Strain Curves for Solid 01 Steel and Solid Purdue Soft Alloy S2.

about 5%. The last figure is lower than one desires to have but it is large enough to have meaningful tests on the alloy complex. Note the stress-strain curves presented here are engineering stress-strain curves. The heavier symbol at the end of each σ-ε curve represents the fracture point.

3.2.2 The Effect of Oxidation Time(Partial Debonding) on Tensile Properties at Constant Fraction Soft Layer.

The fraction of soft layer was chosen to be .50, i.e., equal amounts of hard layer and soft layer, as suggested by the rational method of optimizing the properties of the alloy complex (for detail, see the renewal proposal, Nov., 1973). At this constant soft layer fraction, four sets of specimens were prepared: no oxidation of layers prior to hot-roll welding, 1 hr., 2 hrs., and 3 hrs. oxidation at 600°C.

The σ-ε curves for these four sets of specimens are shown in Figures 7, 8, 9, and 10. The tensile stress (σ_T), 0.1% yield stress (σ_Y), and the plastic strain (ε_p) of these specimens as a function of oxidation time are plotted in Figure 11. The σ_T and σ_Y decrease slowly while the plastic strain increases significantly as oxidation increases. The percent reduction in area also increases with increasing oxidation (Figure 12). These are expected because as the oxidation increases the interface bonding becomes less perfect. The unbonded areas where retained oxide particles reside may serve as a blunt to the approaching crack and may also allow the interface to separate and let the soft layer to deform independently. As a result, the plastic strain and percent reduction in area are increased as oxidations increases. This is also in agreement with the interfacial bonding energy measurement. The small decrease in the strengths, less than a 10% drop as

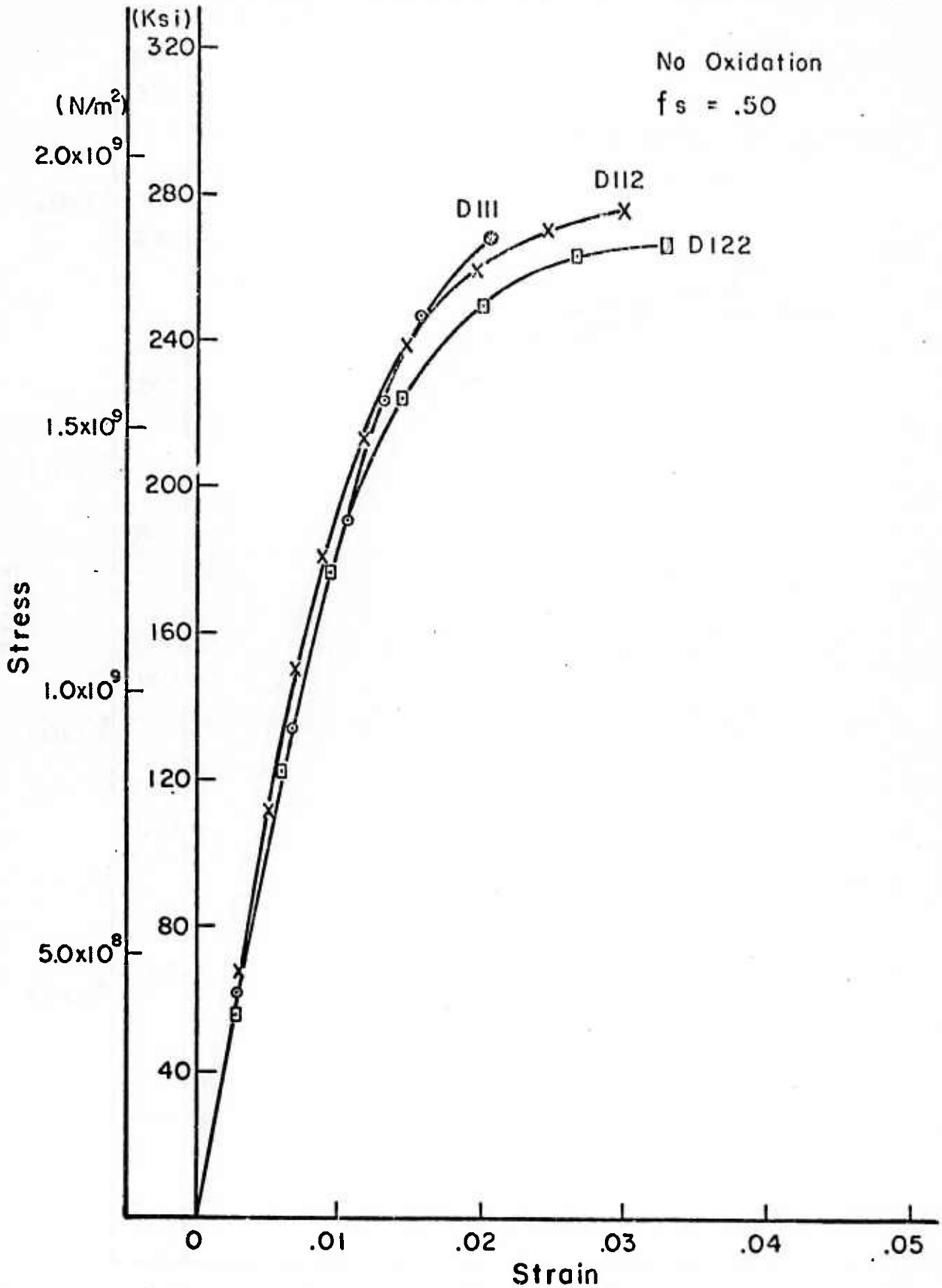

Figure 7. The Stress-Strain Curves for Specimens with No Oxidation Treatment Prior to Hot-Roll Welding.

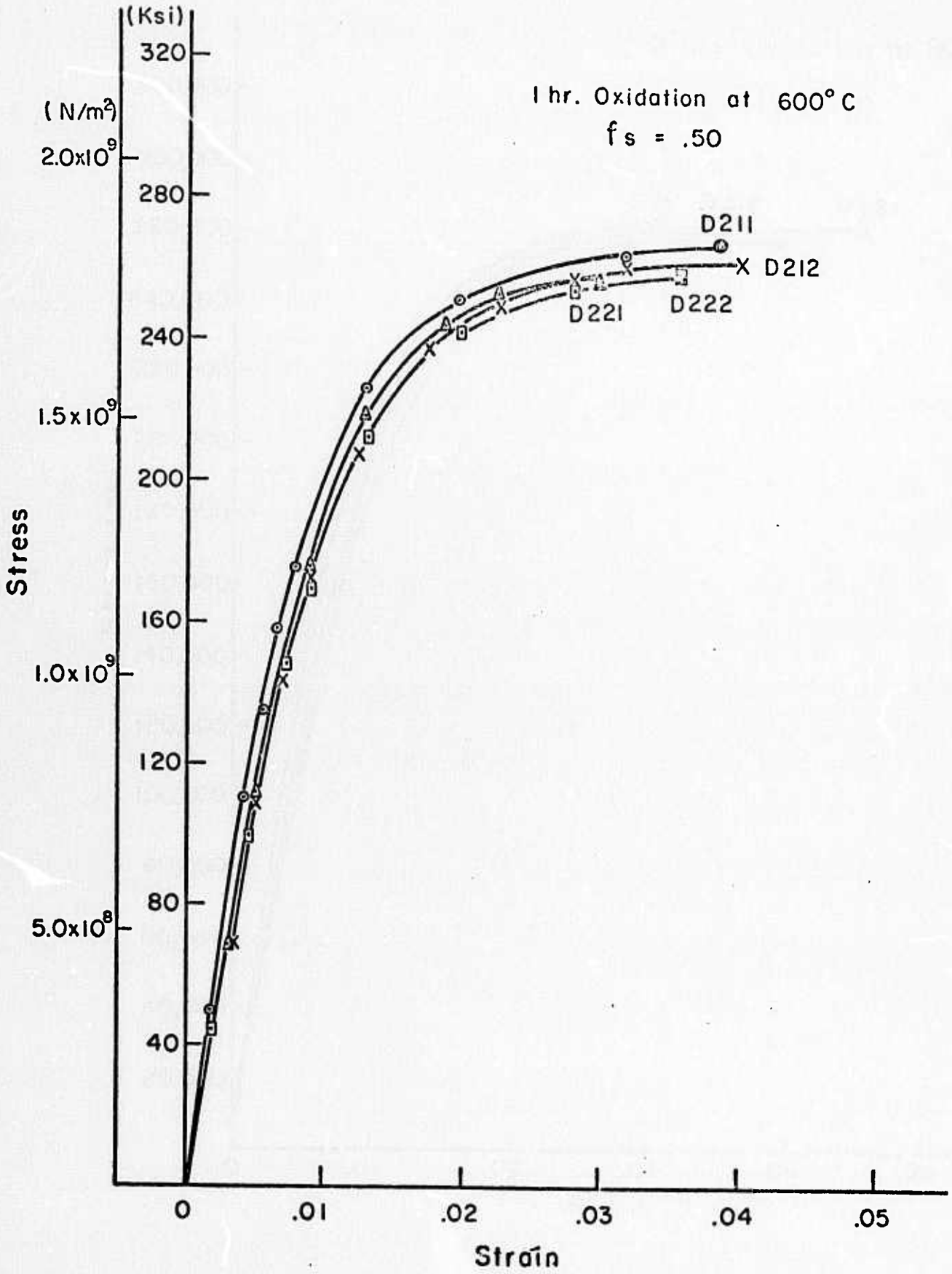

Figure 8. The Stress-Strain Curves for Specimens with 1 hr. Oxidation at 600°C.

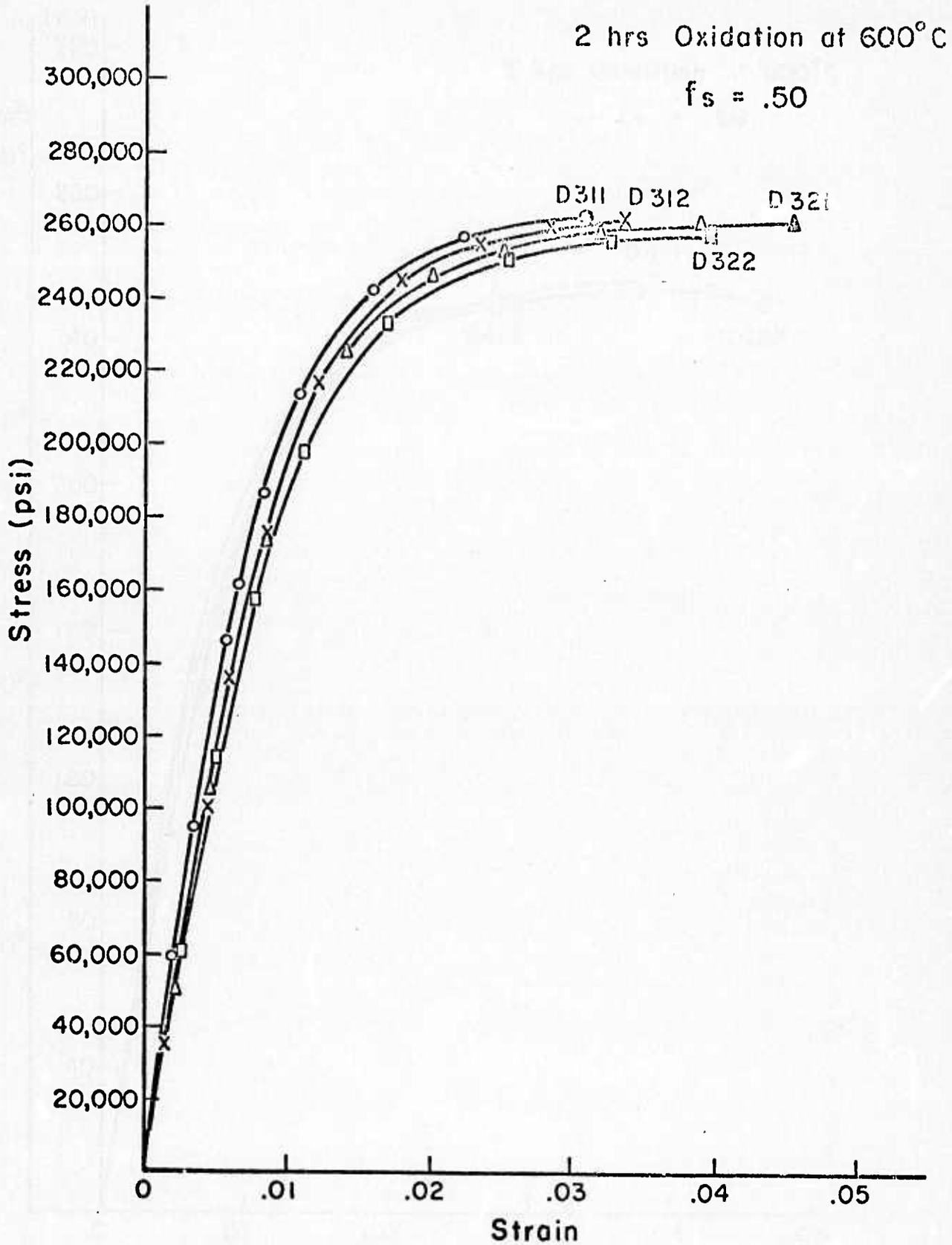

Figure 9. The Stress-Strain Curves for Specimens with 2 hrs. Oxidation at 600°C.

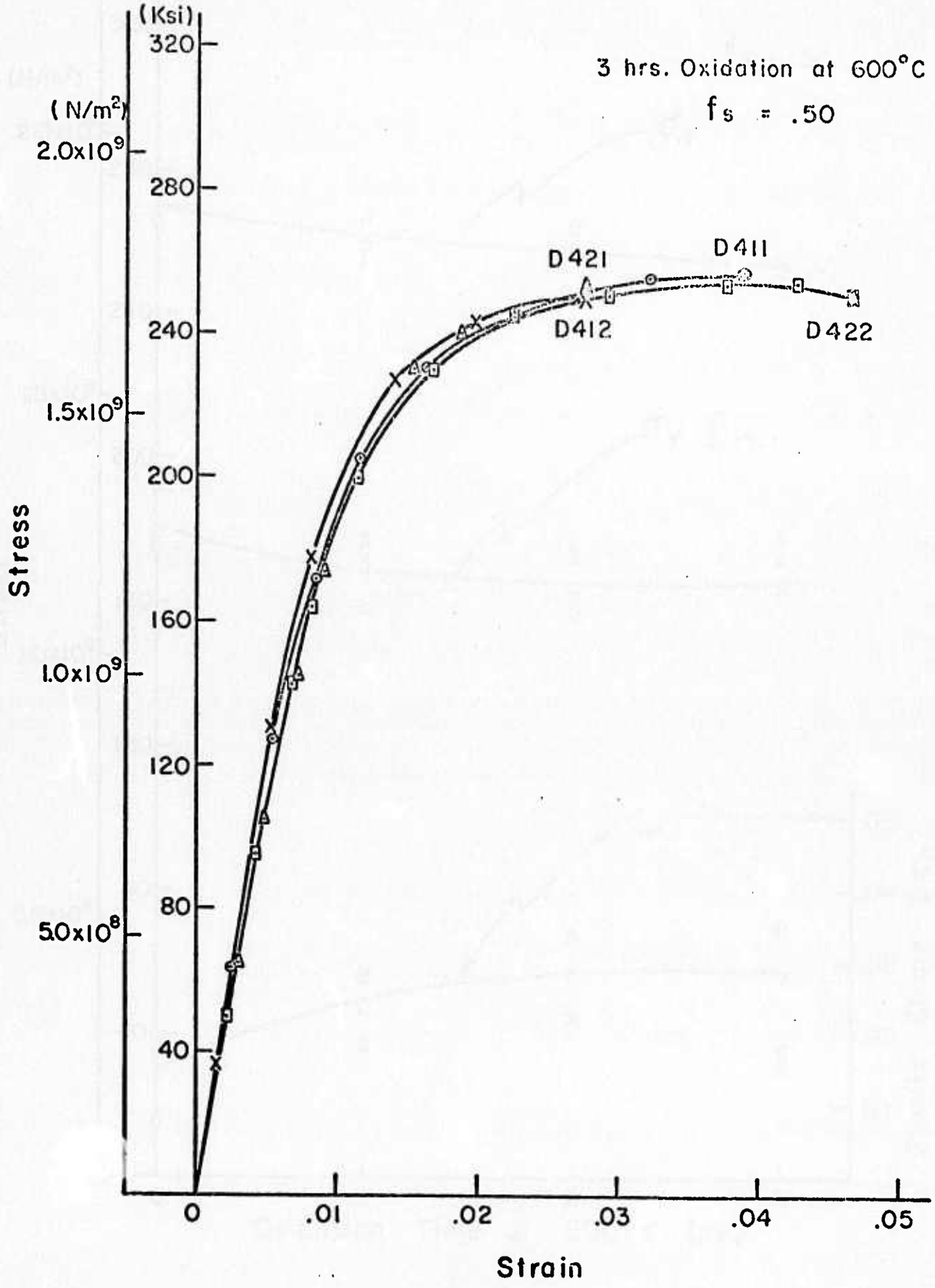

Figure 10. The Stress-Strain Curves for Specimens with 3 hrs. Oxidation at 600°C.

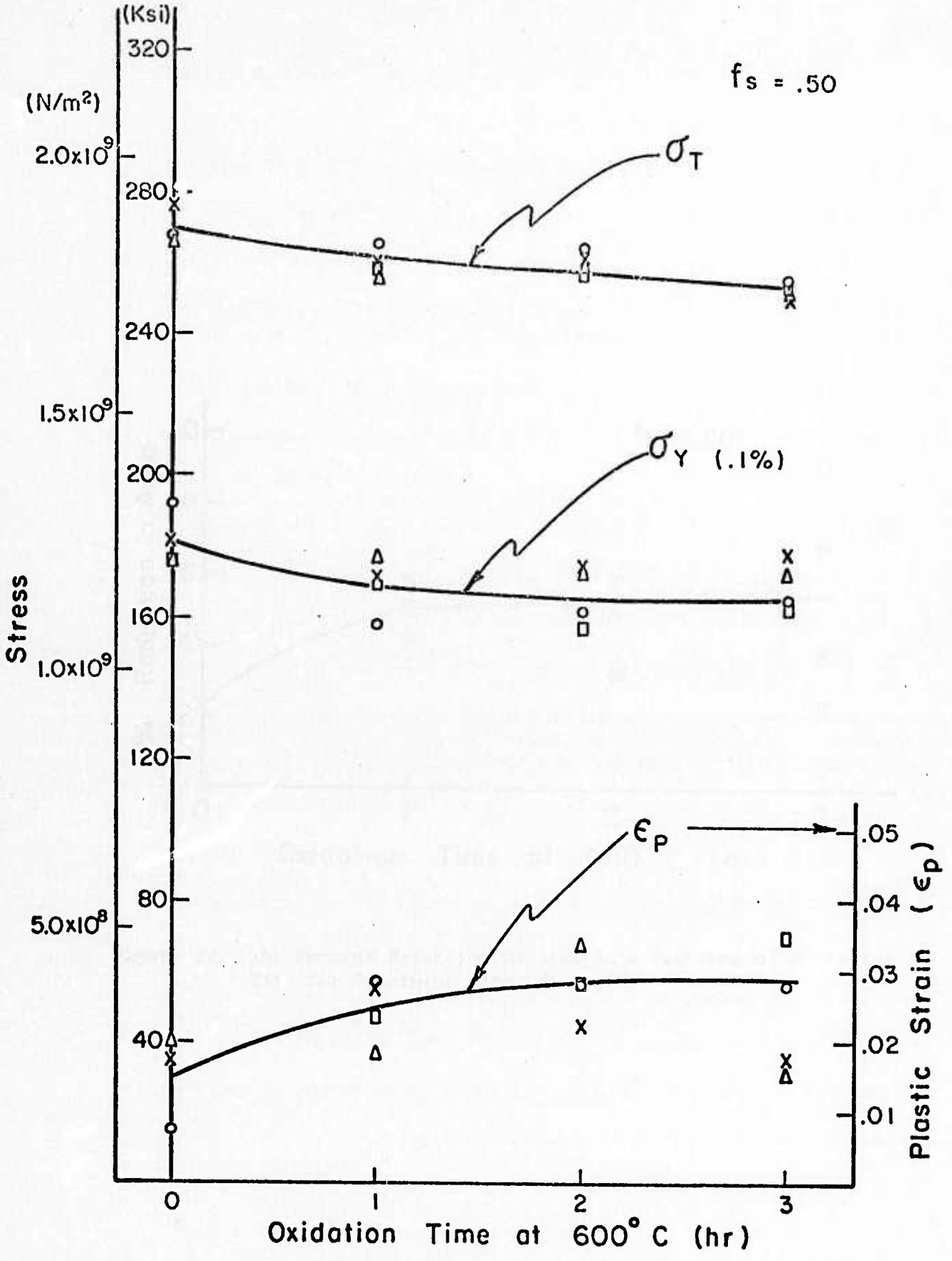

Figure 11. The Tensile Stress, .1% Yield Stress and Plastic Strain As a Function of Oxidation Time for Specimens with fs = .50.

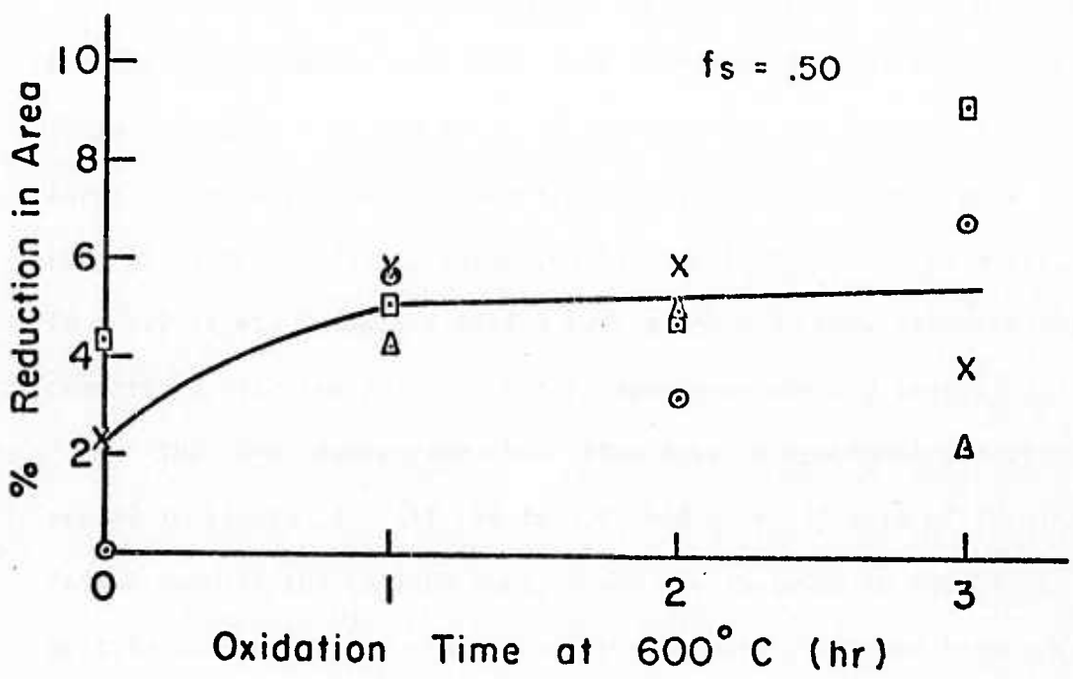

Figure 12. The Percent Reduction in Area As a Function of Oxidation Time for Specimens with fs = .50.

specimens oxidized for 3 hrs., may be due to the slight decrease in effective hard layer volume by decarburization accompanying oxidation. The plastic strain is almost doubled as oxidation time is increased to 3 hrs. The plastic strain increases more rapidly initially and levels off after about 2 hrs. oxidation.

3.2.3 Effect of Soft Layer Fraction on Tensile Properties at Fixed Oxidation Time (Partial Debonding).

Two hours oxidation at 600°C appears to be an optimum treatment for the alloy complex with fs = 0.50 in terms of tensile properties. (Refer to Figures 11 and 12). In order to see the effect of soft layer fraction at this optimum treatment, four additional sets of specimens: fs = 0 (i.e., laminated 01 steel), fs = .25, fs = .75, and fs = 1.0 (i.e., laminated Purdue soft alloy S2), were prepared for comparison with the fs = .50 set of specimens already tested.

The σ-ε curves for these five sets of specimens are presented in Figure 13. All the fs = 0, and fs = .25 sets of specimens failed outside the reduced section and are included to show their brittle nature and the crack jumping phenomena which had been predicted theoretically (renewal proposal [4]). The slope of the elastic portion of σ-ε curves decreases as fs increases. The tensile stress and 0.1% yield stress drop sharply as fs increases (Figure 14). The plastic strain and percent reduction in area increase slowly with increasing fs and rapidly beyond fs = .75 (Figures 15 and 16). The amount of plastic strain as a function of soft layer fraction seems to deviate from the law of mixtures while the strengths of the alloy complex agree well with the law of mixtures.

3.3. Microstructure.

An example of oxide particles retained in the interfacial area is

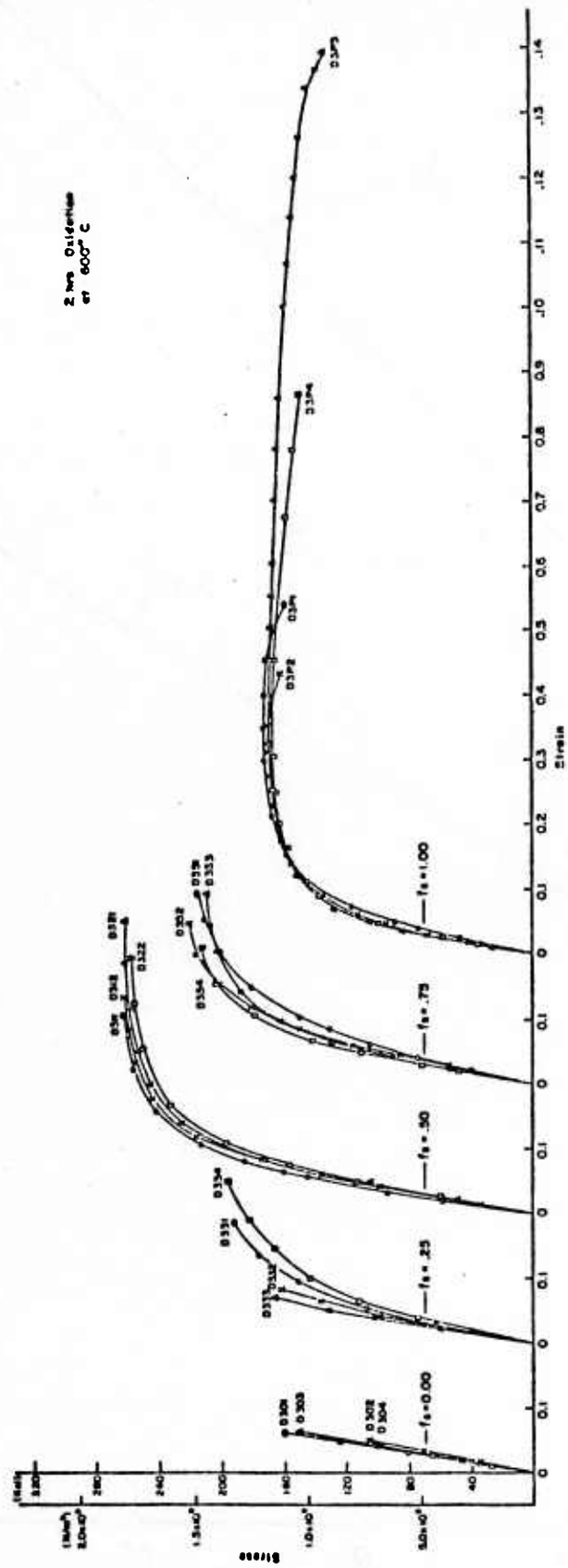

Figure 13. The Stress-Strain Curves for Specimens with fs = 0, .25, .50, .75 and 1.00. All specimens were oxidized at 600°C for 2 hrs. prior to hot-roll welding.

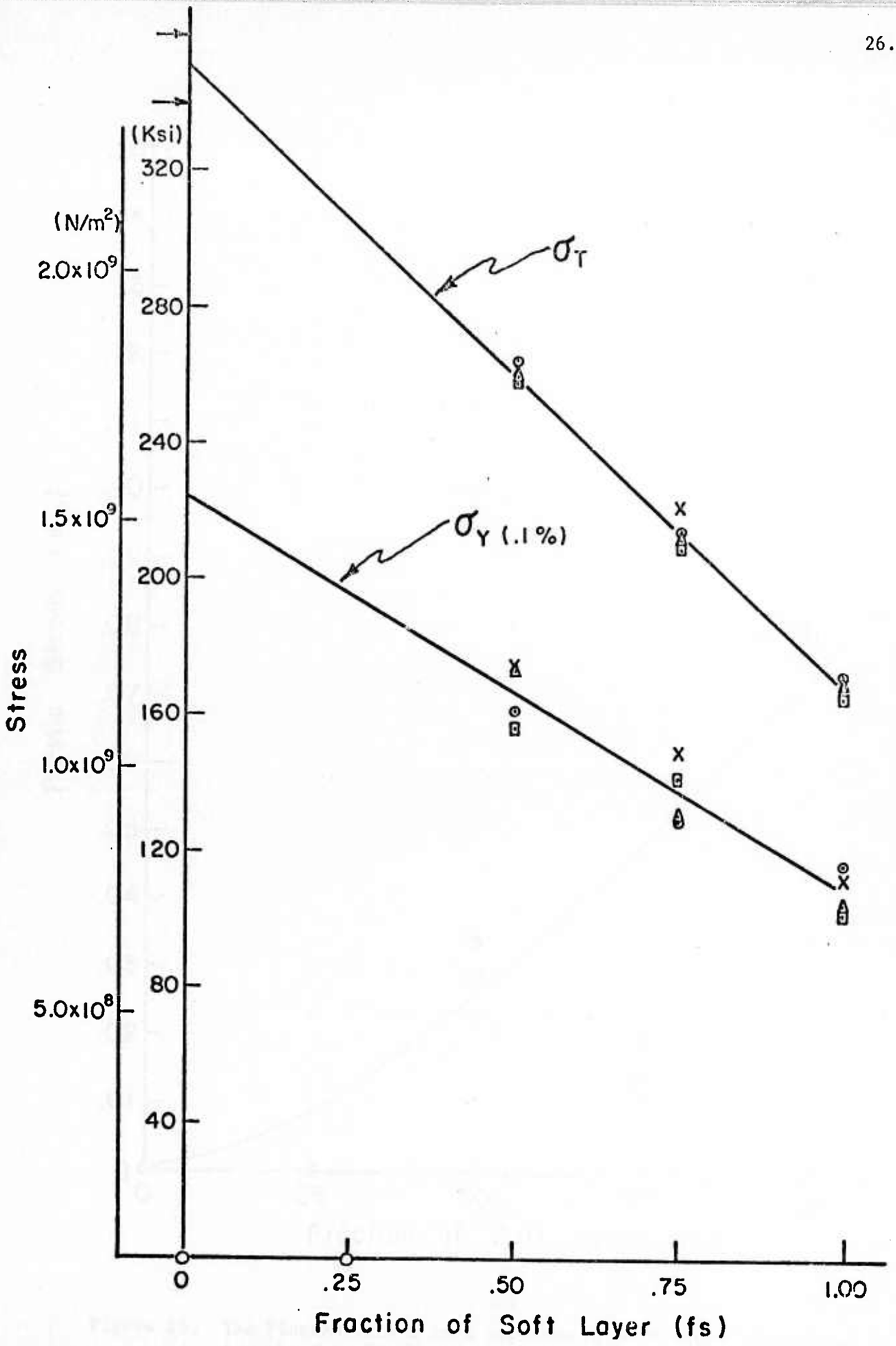

Figure 14. The Tensile Stress and .1% Yield Stress As a Function of Fraction of Soft Layer for the Same Specimens as in Figure 13. Arrows at the upper left corner of the figure represent the upper and lower bounds of 01 steel strength converted from microhardness data.

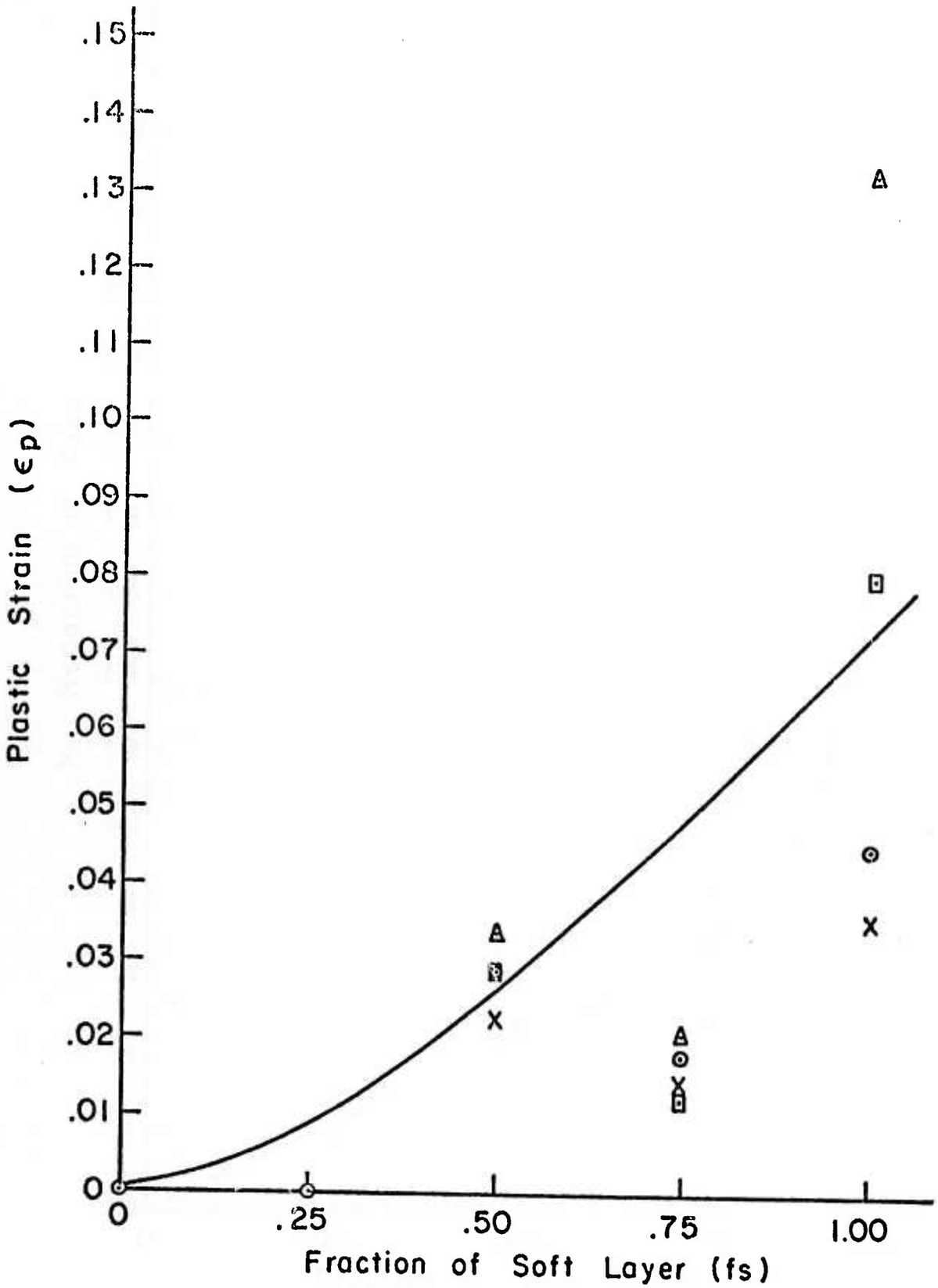

Figure 15. The Plastic Strain As a Function of Fraction of Soft Layer for the Same Specimens as in Figure 13.

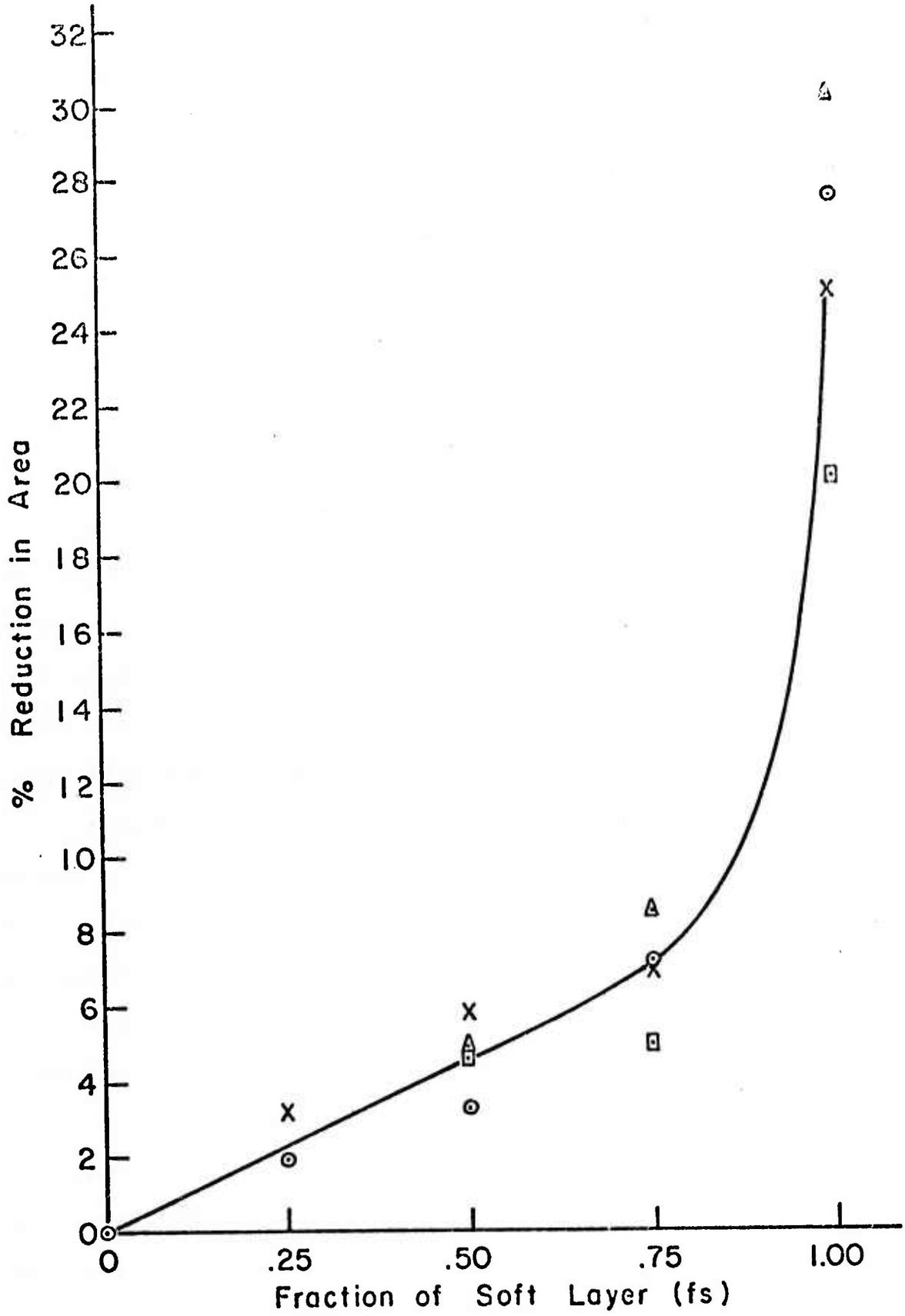

Figure 16. The Percent Reduction in Area As a Function of Fraction of Soft Layer for the same Specimens as in Figure 13.

shown in Figure 17. The nearly circular shape dark particles across the middle of the micrograph are oxide particles. This SEM micrograph with a 3000 magnification was taken on a section of a specimen in which layers were oxidized at 600°C for 30 minutes prior to rolling.

The optical microstructure of the complex has been presented previously[7] but for completeness a low magnification photomicrograph of a complex typical of the present series, i.e., fs = .50 and oxidation treatment 2 hrs. at 600°C, is shown in Figure 18.

3.4. Microhardness.

Tensile specimen D121 was sectioned into five pieces. The outer two parts including pin hole and the central reduced section were mounted and polished for microhardness measurement. Figure 19 shows the Knoop hardness number versus distance modulation direction (i.e., perpendicular to interfaces). The hardness numbers in hard or soft layers alone are quite consistent except two outer soft layers.

The hardness numbers in the hard layers are around 800 while those in the soft layers are about 410. The constant hardness of the soft and hard layers and proper hardness achieved in both prove that the heat treatment was properly performed. The decrease in hardness at the exterior surface of the outer soft layers might be due to the draining of carbon from these layers into the stainless steel container during the hot-roll welding process.

Another hardness measurement sequence was performed on the central hard layer from one end of the tensile specimen D 121 to the other. The results are presented in Figure 20. The Knoop hardness numbers vary from 750 to 800 within each section. This implies that quenching was essentially uniform along length of specimen and again the proper heat treatment was obtained.

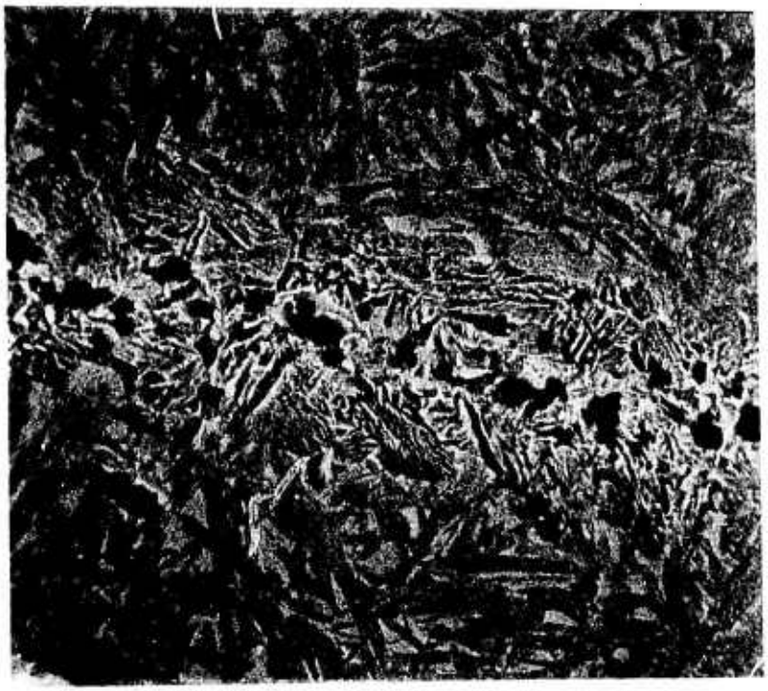

Figure 17. The Microstructure of a Specimen Oxidized at 600°C for 1/2 hr. Prior to Hot-Roll Welding. The dark particles in the central portion of the micrograph are oxide particles. Magnification 3000x.

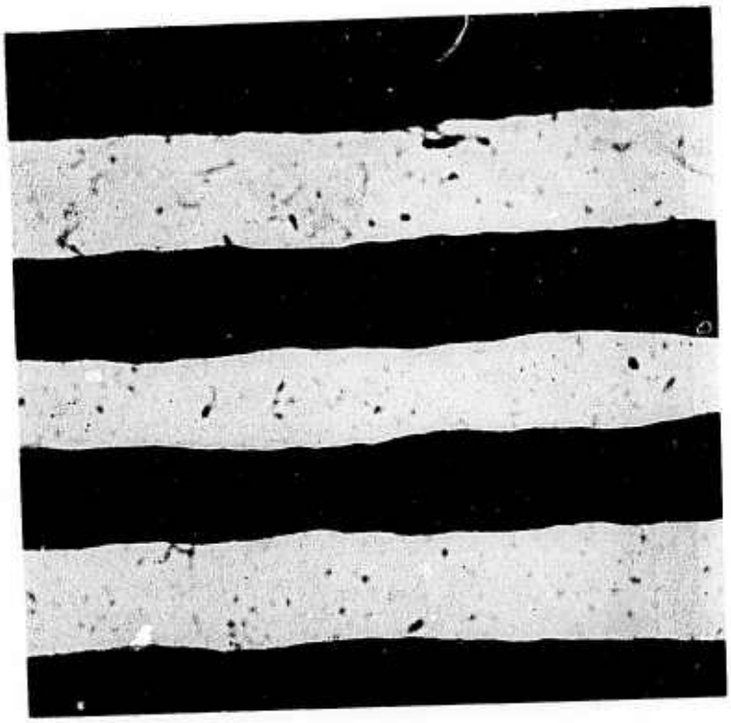

Figure 18. The Microstructure of Specimen D 121. The dark areas represent the hard layer (01 Steel) consisting of fine martensite with a small amount of retained austenite. The light areas are the soft layer (Purdue S2 alloy) in which the martensite appears to have larger plate size. Magnification 80X.

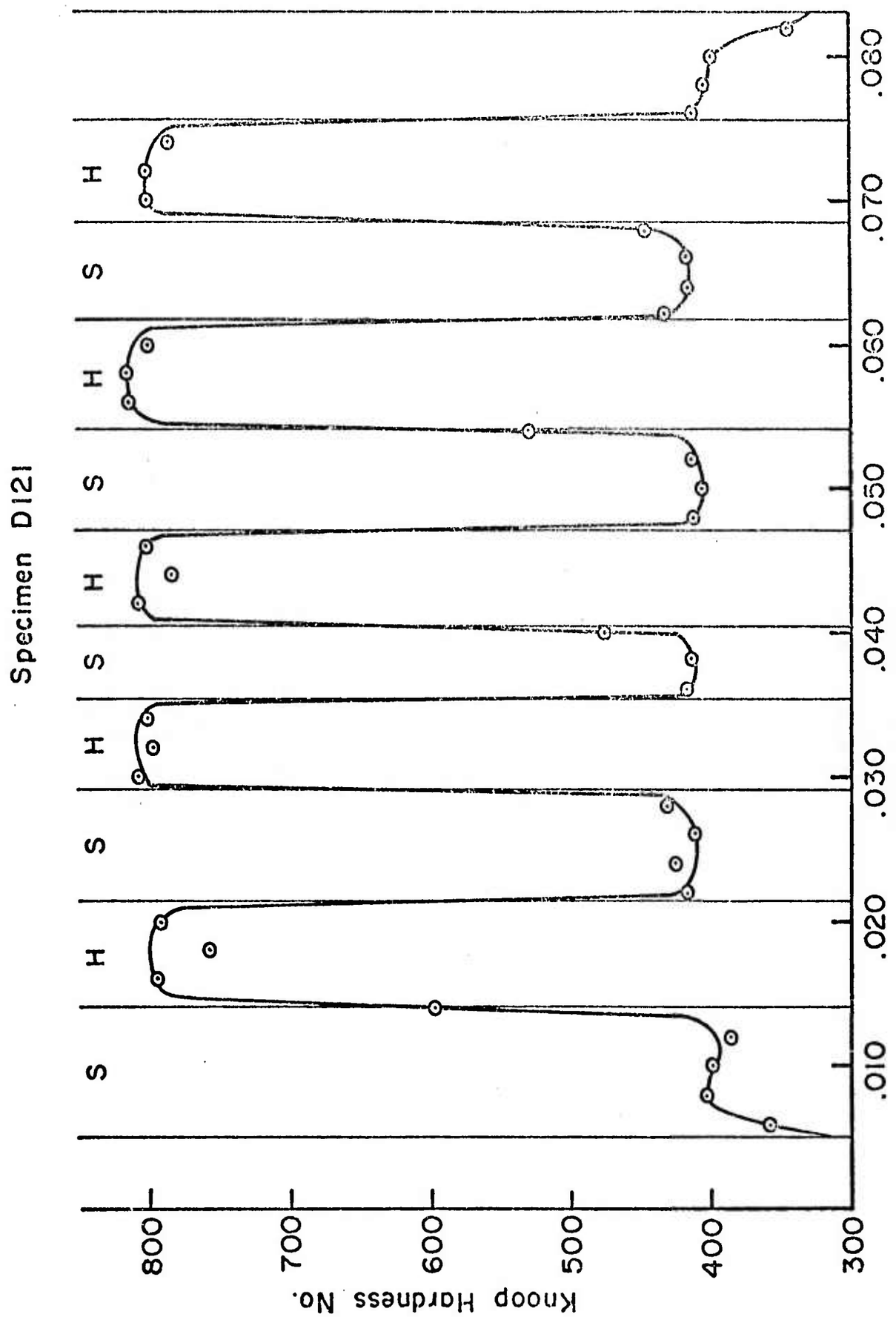

Figure 19. The Microhardness As a Function of Distance in Modulation Direction for Specimen D 121.

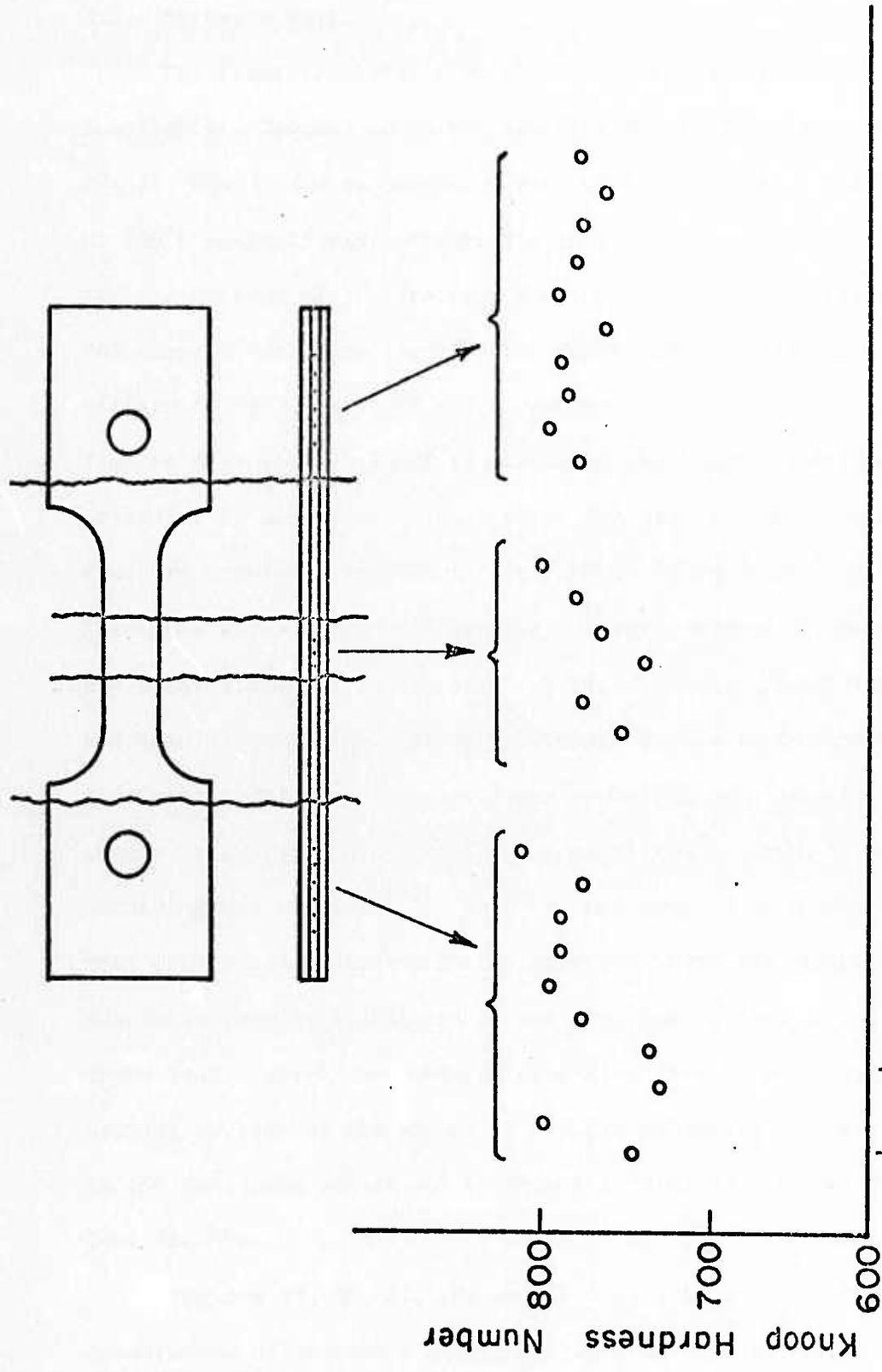

Figure 20. The Microhardness of the Central Hard Layer As a Function of Distance Along the Tensile Axis for Specimen D 121.

3.5. Fracture Path.

The fracture surfaces of all the specimens tested were examined microscopically. Typical schematic fracture topographies are shown in Figures 21, 22, 23, and 24 for no oxidation and for 1 hr., 2 hrs., and 3 hrs. oxidation at 600°C respectively. Figure 21A is a scanning electron micrograph of a typical portion of the fracture shown schematically in Figure 21. Figure 24A shows a corresponding view for Figure 24. The fracture topography differs for that of the Phase I specimens in three ways. Firstly, figures show that in Phase II specimens the overall fracture surface is irregular in appearance except for a few hard layers where brittle fracture occured. In contrast, the Phase I specimens[7] produced smooth fractures which distinctly brittle fracture occured in the hard layers and shear fracture in the soft layers. Secondly, debonding along interfaces and some degree of necking of individual layers is present in the Phase II specimens. This is direct evidence of having more plastic strain in these specimens compared with the Phase I specimens in which no necking and no debonding was observed[7]. Thirdly, the origins of cracks in these specimens were usually located in the interior while the cracks in Phase I specimens usually originated at the exterior surface of a hard layer. These four figures show that as oxidation time is increased, the amount of necking as well as the amount of partial debonding increases. This results in the increased strain and reduction in area as observed in the tensile test results.

Figures 25, 26, 27, 28, and 29 show schematically the fracture appearances of specimens D 304, D 332, D 312 (which is repeated from Figure 23 for comparison), D 353 and D3P4. These specimens were all oxidized for 2 hours and show soft layer contents which range from zero to one. Figures 25A, 26A, 27A, 28A, and 29A are scanning electron micrographs

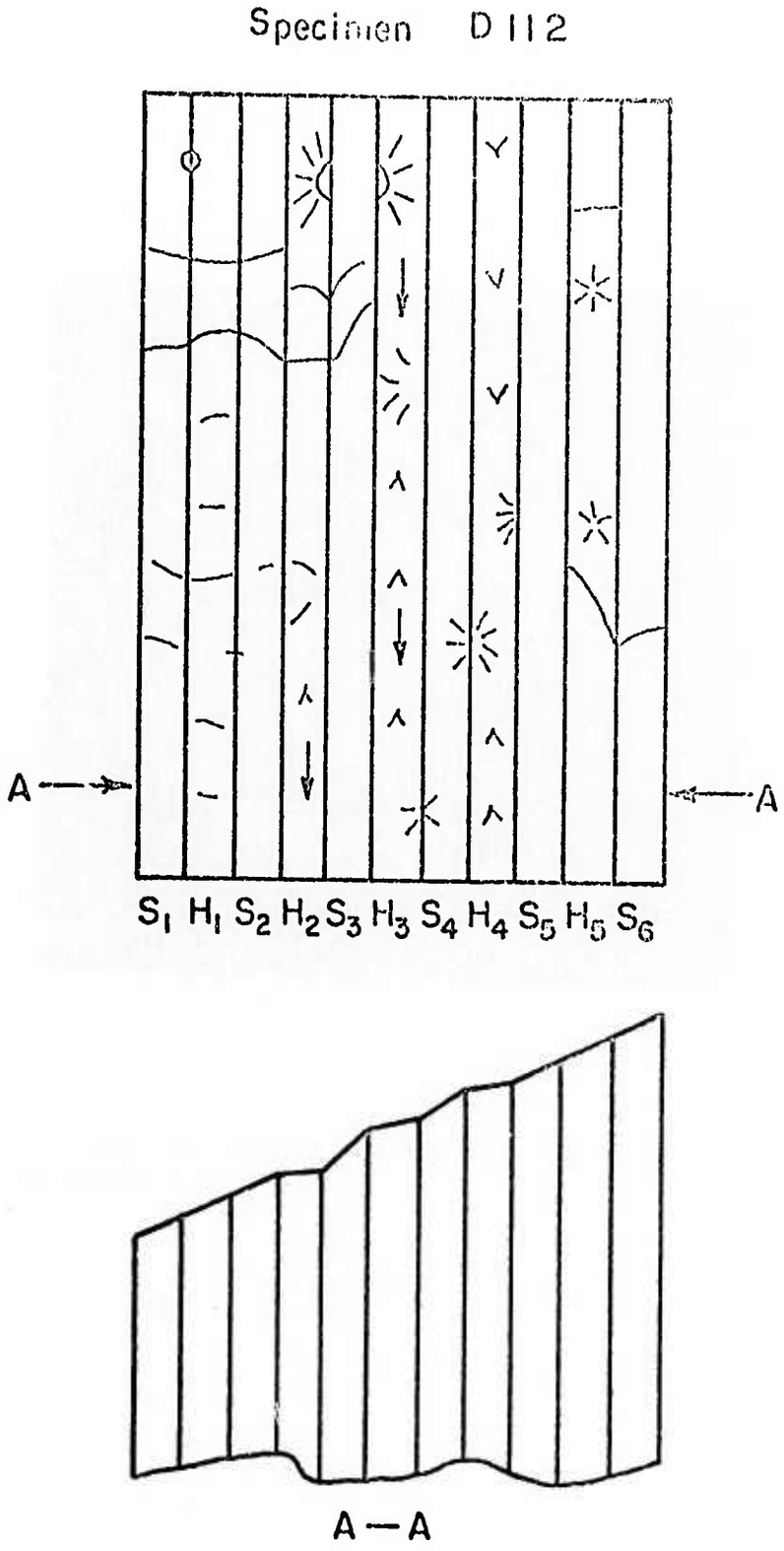

Figure 21. A Schematic Fractograph for Specimen D 112. The crack originated from H_2, S_3, and H_3 area. The shear fracture modes dominated except in H_2, H_3, and H_4 where brittle fracture occured. No debonding or necking was observed.

Figure 21A. A Micrograph Showing the Fracture Surface of Specimen D 112. Magnification 100x.

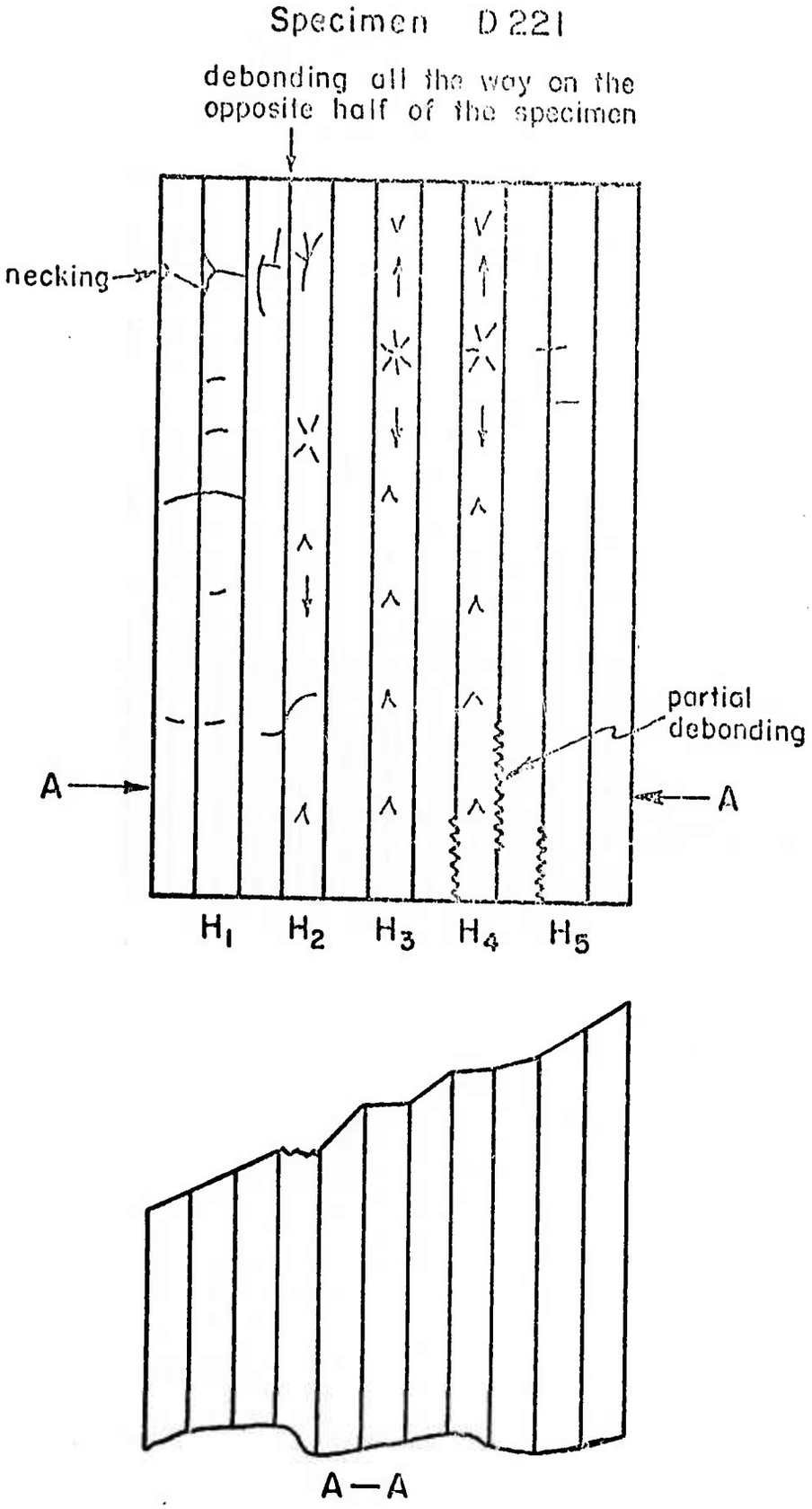

Figure 22. A Schematic Fractograph for Specimen D 221. Again shear fracture modes dominated except in H_3 and H_4, some small amount of debonding was observed.

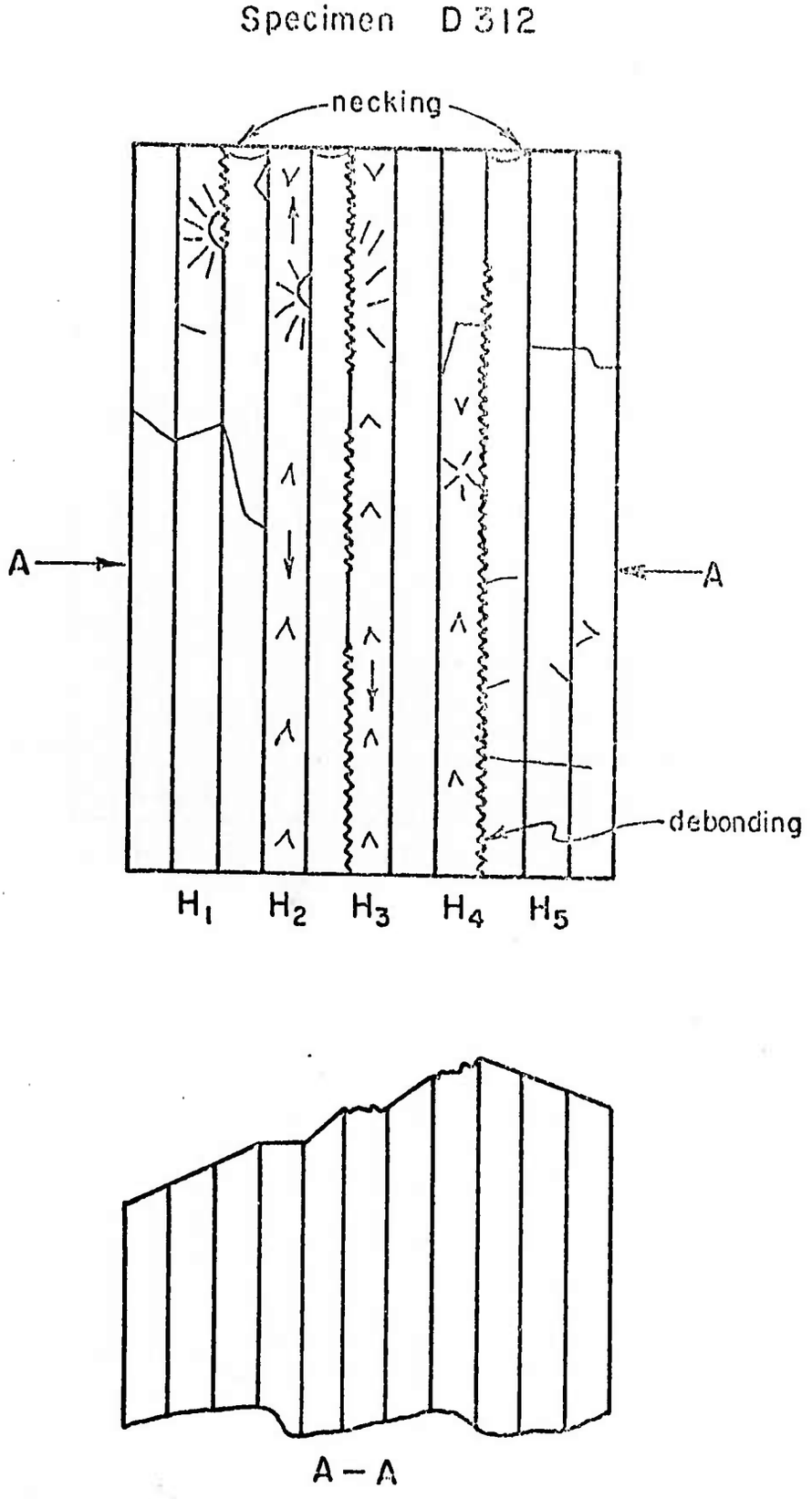

Figure 23. A Schematic Fractograph for Specimen D 312. Except flat brittle fracture in H_2 and H_3, the shear fracture modes were observed. Some neckings at edge and more partial debonding were observed. Crack originated from either H_1 or H_2.

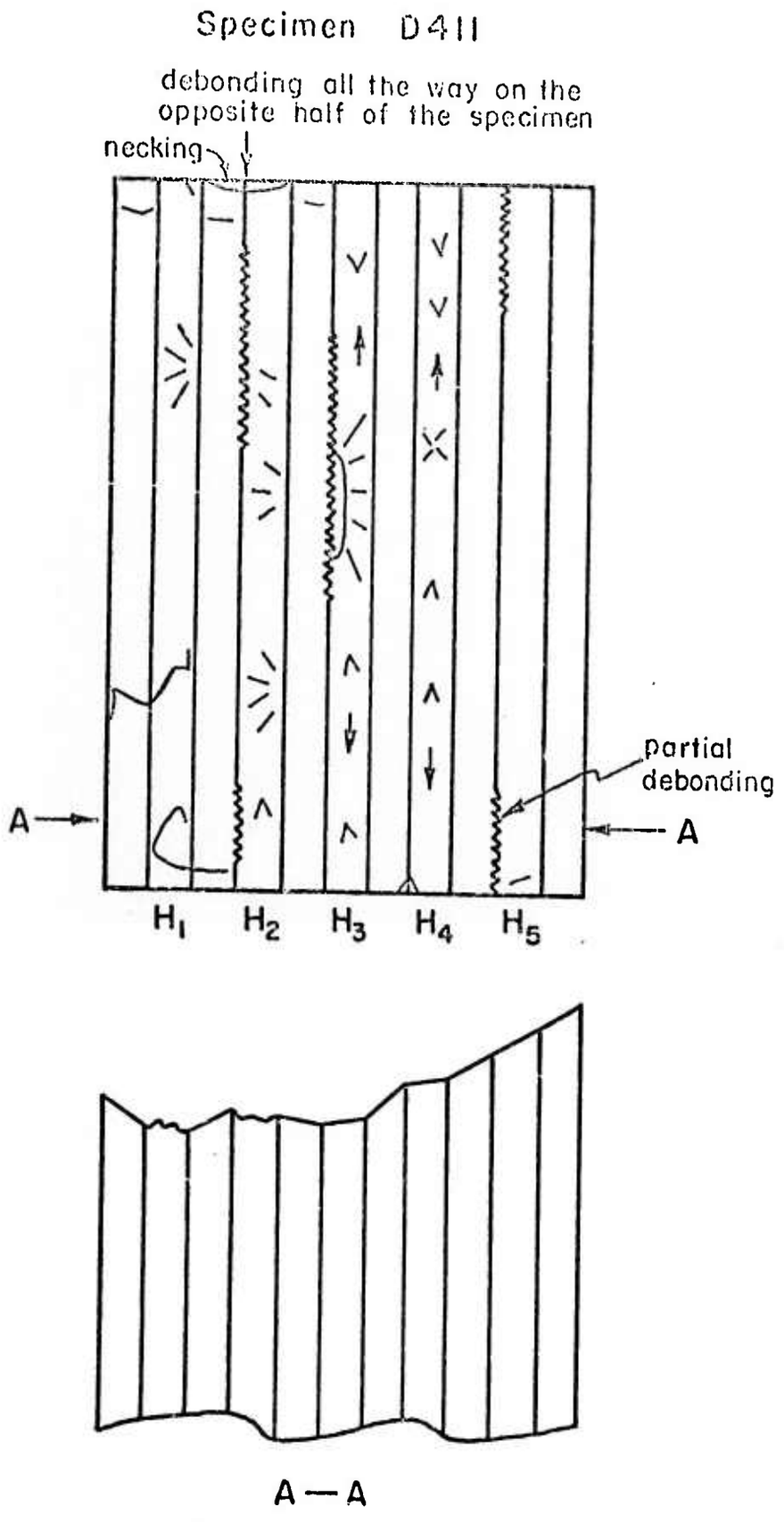

Figure 24. A Schematic Fractograph for Specimen D 411. There are more typical cone and cup tensile fracture characteristics at edges, more debonding. Shear fracture modes were observed except H_3 and H_4. The crack originated from the central portion of H_3.

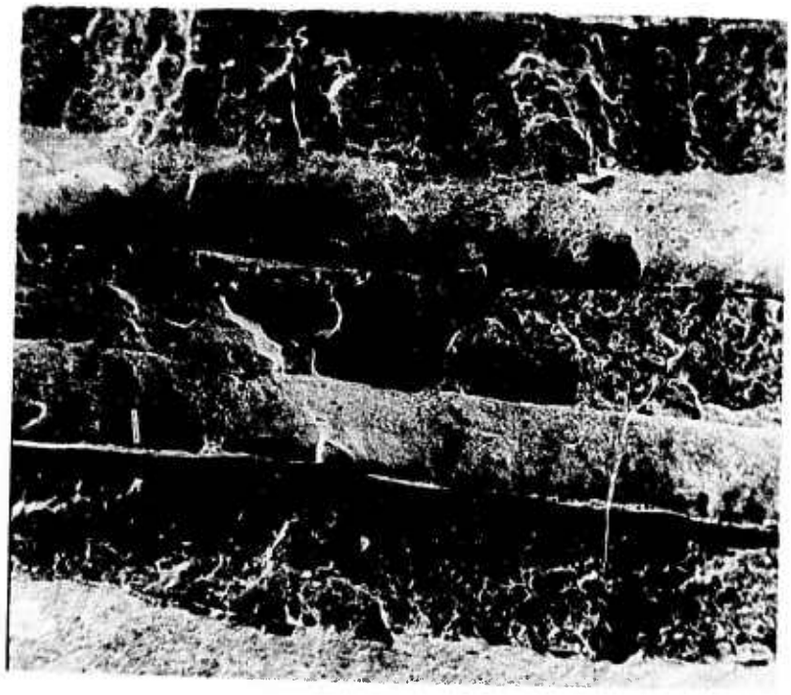

Figure 24A. A Micrograph Showing the Fracture Surface of Specimen D 411. Magnification 100x.

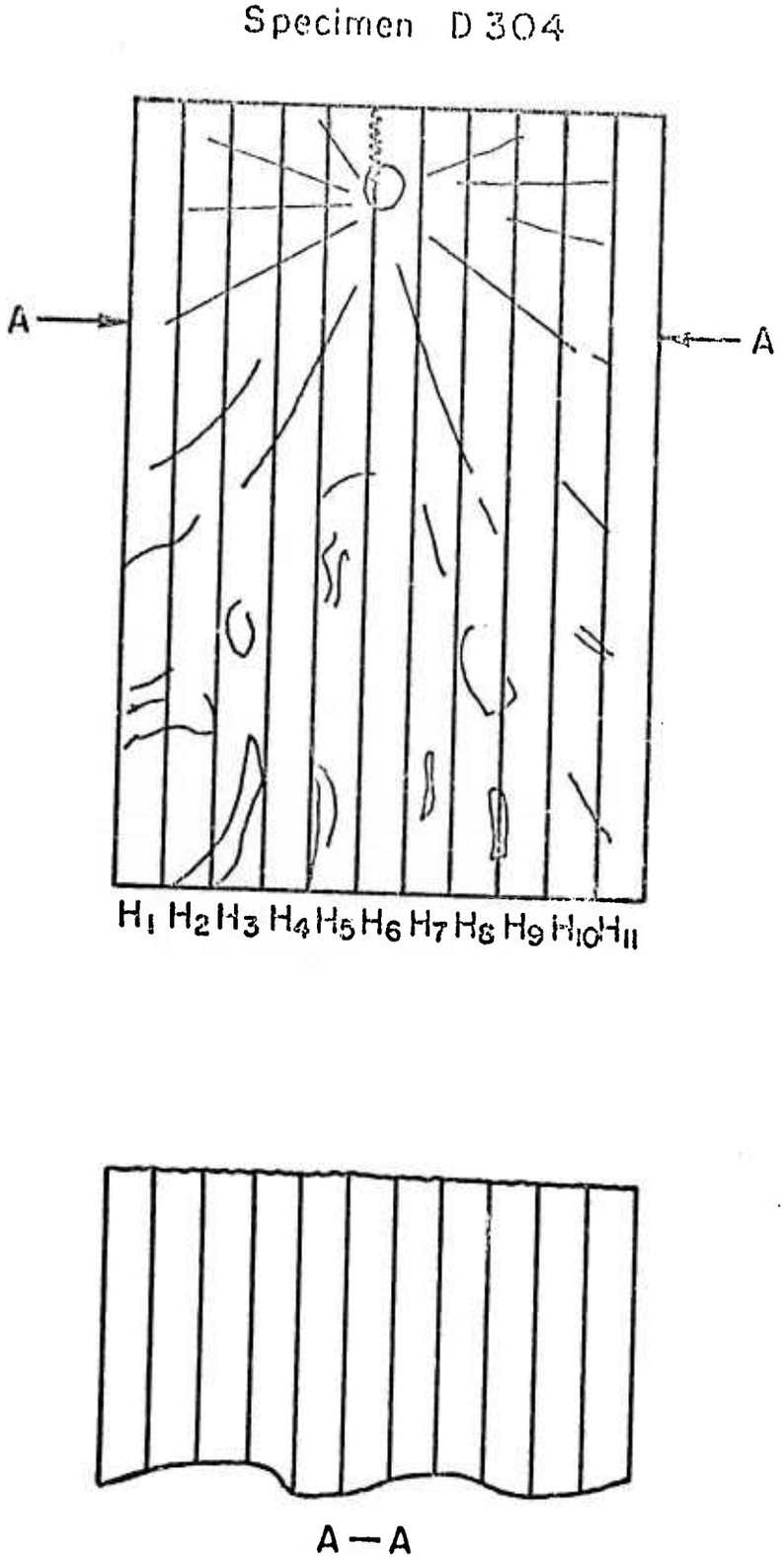

Figure 25. A Schematic Fractograph for Specimen D 304 ($f_s = 0$). Crack originated from the interface between H_5 and H_6. Brittle fracture occured in the upper half of the specimen and shear dimple type in the lower half. The interfaces were indistinguishable.

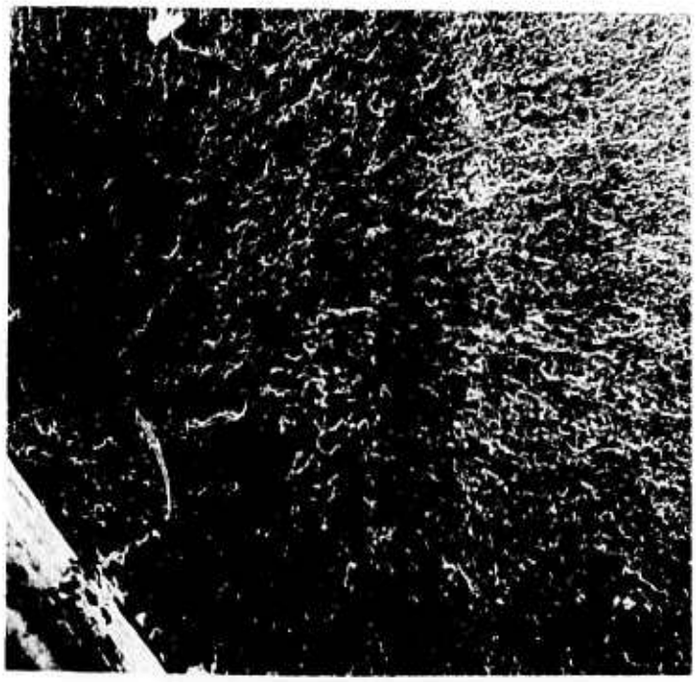

Figure 25A. A Micrograph Showing the Fracture Surface of Specimen D 304. Magnification 100x.

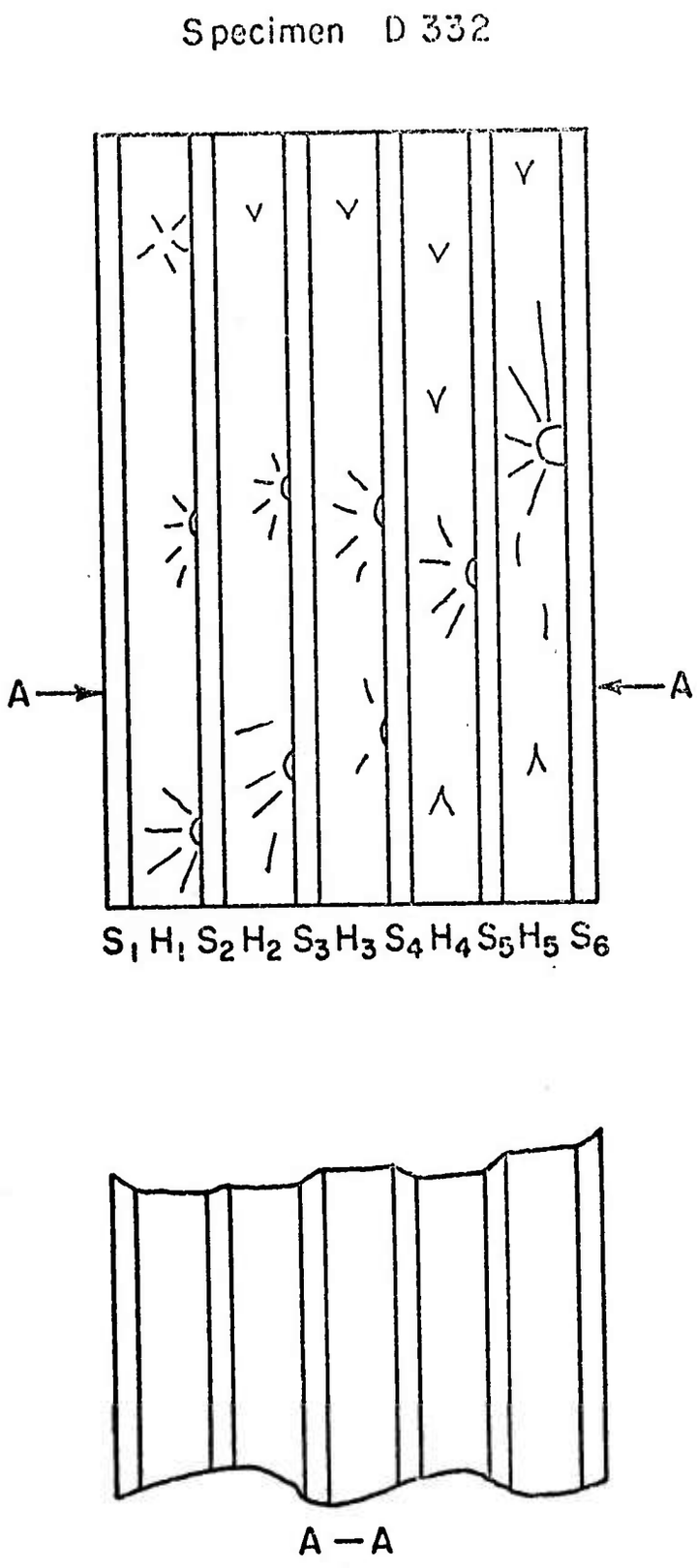

Figure 26. A Schematic Fractograph for Specimen D 332 (fs = .25). Brittle fracture occured in hard layers and shear fracture occured in soft layers. Crack originated from H_2 propagating to the left of the specimen. Multiple crack nucleation sites were observed in hard layers.

Figure 26A. A Micrograph Showing the Fracture Surface of Specimen D 332. Magnification 100x.

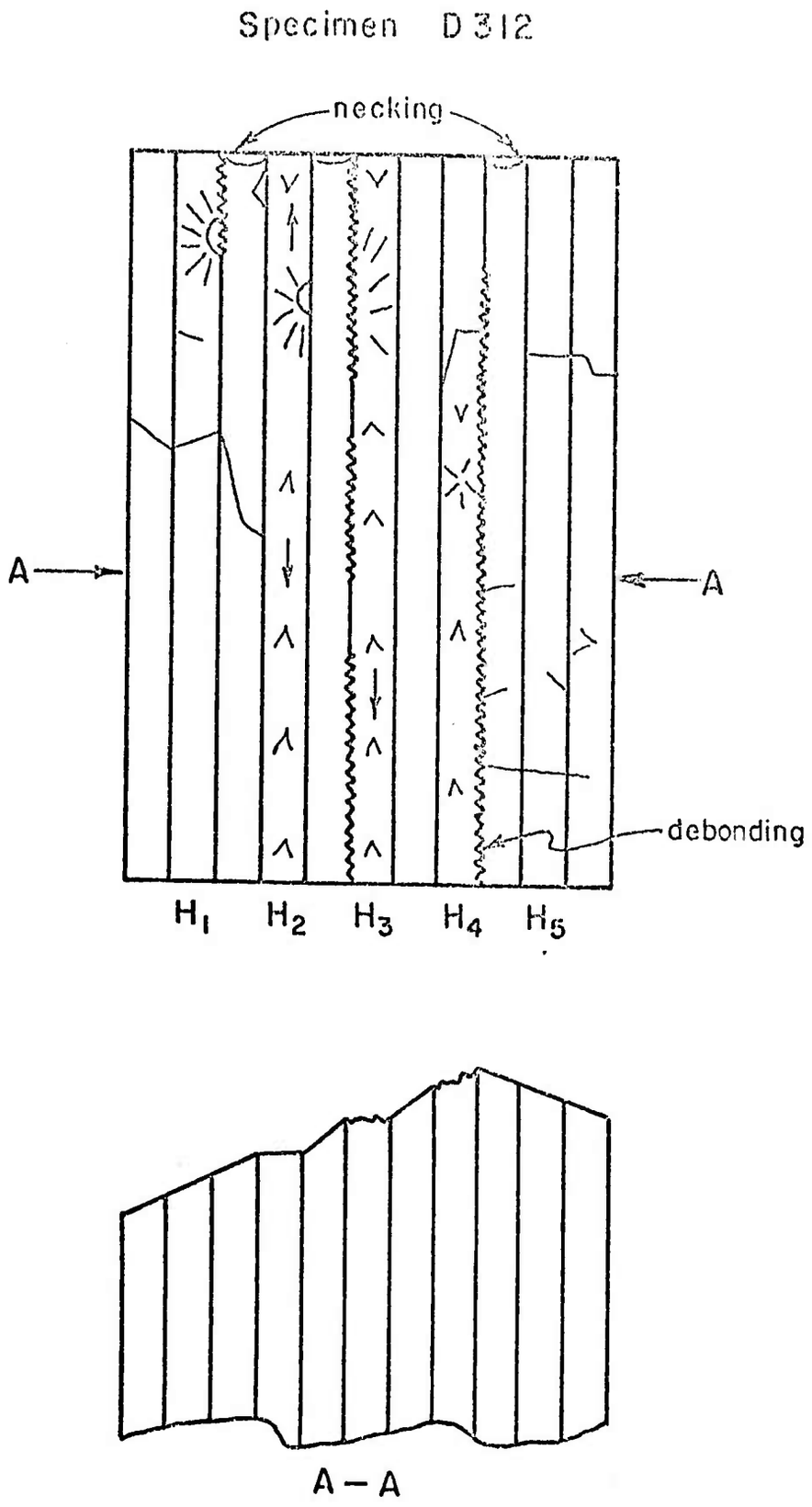

Figure 27. A Schematic Fractograph for Specimen D 312 (fs = .50). Repeated from Figure 23.

Figure 27A. A Micrograph Showing the Fracture Surface of Specimen D 312. Magnification 100x.

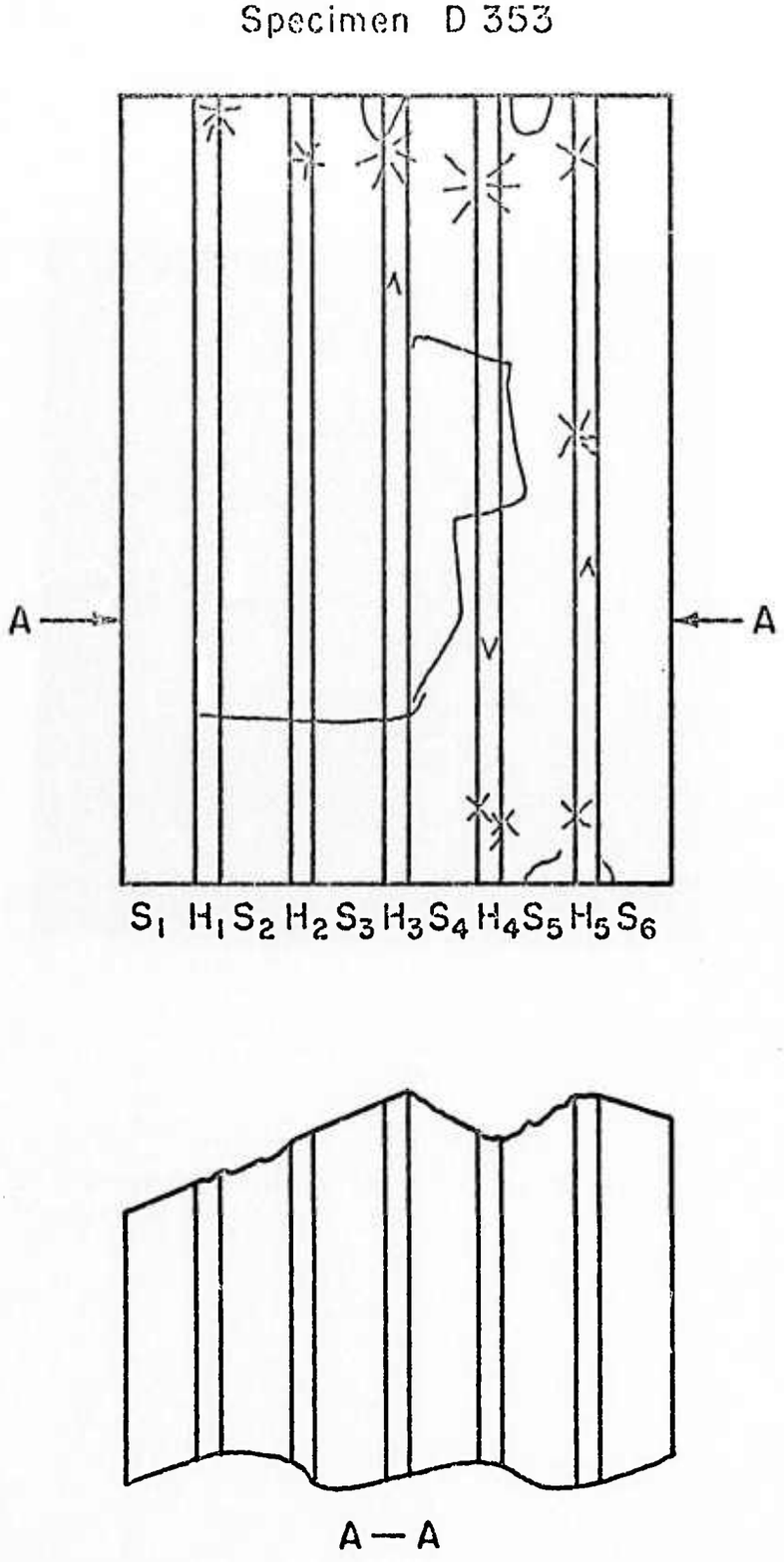

Figure 28. A Schematic Fractograph for Specimen D 353 (fs = .75). Except H_5, mostly shear fracture modes were observed. Crack originated from the upper portion of the specimen, most likely H_4.

Figure 28A. A Micrograph Showing the Fracture Surface of Specimen D 353. Magnification 100x.

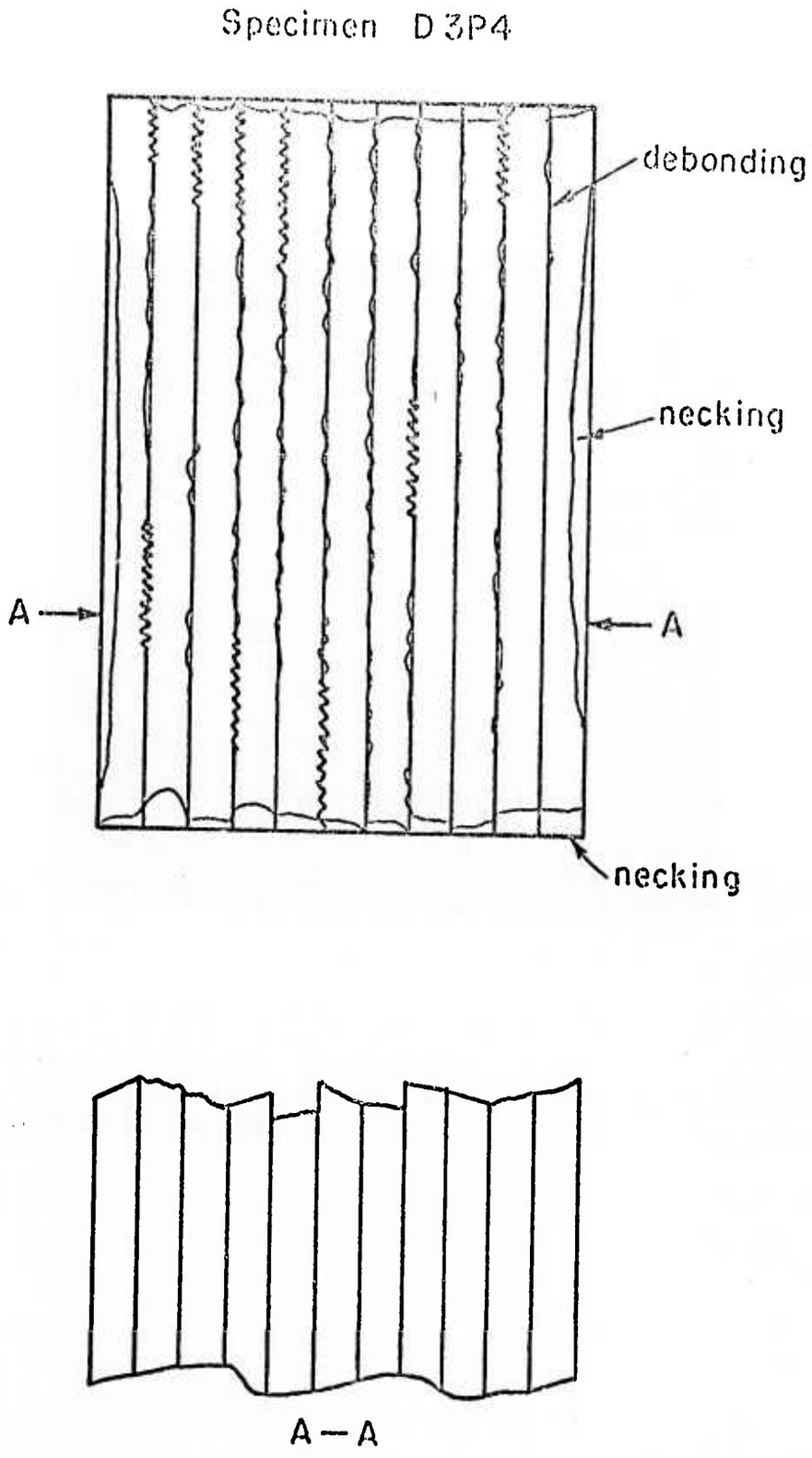

Figure 29. A Schematic Fractograph for Specimen D3P4 (fs = 1.00). Exclusively ductile shear fracture occured in this specimen. There was about 95% debonding and large amount of necking observed.

Figure 29A. A Micrograph Showing the Fracture Surface of Specimen D3P4. Magnification 100x.

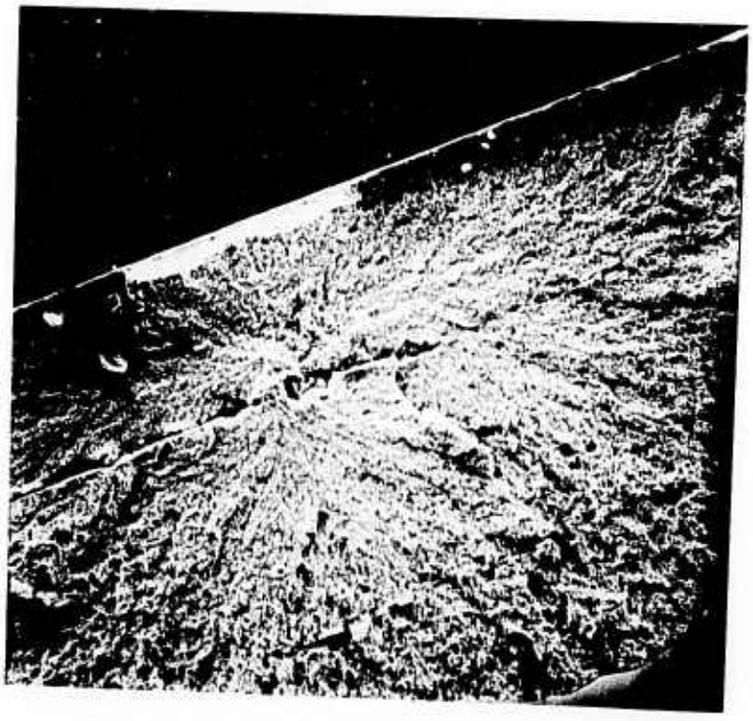

Figure 30. A Micrograph Showing the Origin of a Crack in a Solid 01 Specimen. Magnification 100x.

of the portions of the fractures shown in Figures 25, 26, 27, 28, and 29. The fracture in the laminated 01 steel (Figure 25) shows typical brittle fracture characteristics. For specimens with fs = .25 (Figure 26), the crack nucleation sites as it propagated across the whole specimen. This is similar to the fracture behavior of Phase 1 specimens. As fs is increased, Figures 27 and 29, the degree of debonding and necking increases and so does the amount of shear fracture. Figure 28 shows reduced debonding and necking and the corresponding tensile tests show decreased ductility but not decreased area reduction. The reason for this exceptional behavior is not clear.

In contrast to the scanning electron micrographs of fractures of laminated complexes, the fracture of the solid 01 and solid Purdue S2 alloy are both smooth and perpendicular to the tensile axis. These are shown in Figures 30 and 31.

IV. Conclusions.

A Purdue soft layer alloy S2 has been designed based on several design criteria to match the hard layer alloy, AISI type 01 tool steel. The S2 alloy was successfully fabricated with a vacuum melting facility at crystal growing laboratory of Purdue University. The ingots were hot-rolled to suitable size for manufacturing of alloy complex (MMS) with 01 steel.

One of the most important conclusions in Phase I study was that the interfaces were too well bonded. As a result, the soft layers could not deform independently and little ductility was observed. The idea of the necessity of having partial debonding in interfaces was generated. In Phase II, a technique of creating partial debonding in interfaces by oxidation of the surfaces of layers prior to hot-roll welding has been developed and evaluated. A method of interfacial bonding energy measurement was developed to characterize the interface

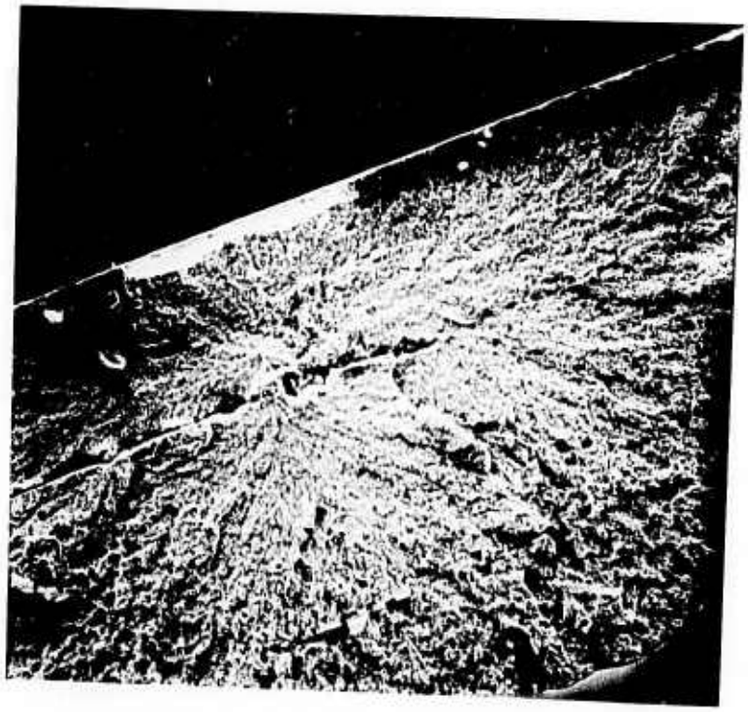

Figure 30. A Micrograph Showing the Origin of a Crack in a Solid 01 Specimen. Magnification 100x.

Figure 31. A Micrograph Showing the Origin of a Crack in a Solid Purdue S2 Specimen. Magnification 100x.

bonding and preliminary measurements were made which show that the energy decreases as the oxidation time increases.

The partial debonding resulted from the retained oxide particles in interfaces contribute ductility to alloy complex as had been theorized. The evidence is shown in the study of the effect of oxidation time on the tensile properties of alloy complex at 50% soft layer fraction. In that study, the tensile stress and .1% yield stress decrease slowly with increasing oxidation time, while the plastic strain increases rapidly as oxidation increases which is in agreement with interfacial bonding energy measurement.

In the case of the effect of soft layer fraction on the tensile properties of alloy complex at constant oxidation time, i.e., identical debonding condition, the results show: (1) the tensile stress (σ_T) and .1% yield stress (σ_Y) drop sharply as fs increases. (2) σ_T and σ_Y of the alloy complex obey the law of mixture well. (3) the plastic strain and the percent reduction in area increase slowly with increasing fs and rapidly beyond fs = .75 which seems to deviate from the law of mixtures.

The examination of fracture surfaces revealed that the shear fracture modes dominate except in few hard layers where brittle fracture occurred for specimen. of 50% soft layer. The fracture topography was much more irregular compared with that of Phase I specimens. There were more partial debonding and more necking which implied more plastic strain as oxidation time was increased. This agreed with the tensile test results quite well.

Another interesting observation was that the failure in Phase II specimens originated mostly from interior rather than from the edge of one hard layer as occurred in Phase I specimens. This suggests that the replacements of hard layers by soft ones on the outermost layers eliminates the possibility of specimen failure from surface flaws.

V. Summary.

The object of the work is to develop an alloy complex which combines high strength and significant fracture toughness. The basic concept is to alternate layers of high-strength martensite with tough and softer austenite in a complex which can be hardened to strength of 400 Ksi (2.8 GN/m^2) and softened for fabrication by conventional heat treatment.

This development can best be viewed against the presently available mechanical properties of alloy steels. These properties are summarized by Lange[1] as presented in Figure 1. His estimate of the high strength technological limit of fracture toughness is substantially less than 100 $Ksi\sqrt{in.}$ (.11 $GN/m^2\sqrt{m}$) at stress levels in excess of 300 Ksi (2.1 GN/m^2). The proposed alloy should obtain a strength of 400 Ksi (2.8 GN/m^2) and has a target fracture toughness of 150 $Ksi\sqrt{in.}$ (.16 $GN/m^2\sqrt{m}$). This represents a technologically attractive design objective and work is proceeding toward it.

Since the beginning of work on June 1, 1973, a theoretical strategy has been developed based on a preliminary (Phase I) experimental program, and following that strategy a model alloy complex was designed and tested (Phase II). In the Phase I experimental program a technique of fabricating the alloy complex has been developed and some preliminary complexes have been produced and tested. On the basis of the properties observed, a rational method of optmizing the strength and toughness of the alloy complex has been formulated. The theory underlying this method was tested and broadly supported by the alloy complex designed, fabricated, and tested in the Phase II experimental program now nearly complete. Phase I experiments and the theoretical strategy were reported in the First Semi-annual Technical Report[7] and the present report concentrates on the results of the Phase II experimental program.

During the coming year, a new alloy complex will be designed, produced in some quantity (about 50 pounds) and tested as Phase III of the project.

The new complex will have a significantly stronger hard-layer component, and a new soft-layer alloy specially designed to be compatible with the hard layer. The interlayer bonding and the relative layer thickness which were important variables in the Phase II study, will be carefully controlled at new optimum levels based on Phase II experiments and theoretical estimates. We hope that Phase III will result in achieveing the target fracture toughness and strength.

The preliminary experimental program (Phase I) may be broken down into several interdependent parts which are reported in detail in the Semi-annual Technical Report[7]. The fabrication technique consists of hot-roll welding a stack of alternating layers of soft and hard alloy encapsulated in a stainless steel container. The trial system was comprised of readily available tool steels selected so that at room temperature the soft layer contained up to 100 percent austenite whereas the hard layer was nearly all martensite. The soft layer occupied about one-third of the complex. Several tentative conclusions have been drawn from the mechanical property measurements. The most important of these was the observation that fracture crossed the soft layers by renucleation of a crack in the next hard layer and the soft layer itself failed in shear without exhibiting much deformation because deformation of the soft layer is limited by its strong bonding to the neighboring layers. This was apparently the primary cause of the absence of measurable ductitity in the Phase I complexes.

The method of optimizing the fracture and strength properties of the complex was developed based on the observations summarized above. Two basic problems are distinguished: first, the necessity of allowing the soft layer to deform independently, and second, the necessity of making the soft layer thick enough relative to the hard layer so that cracks through one hard layer cannot produce cracking in the next hard layer without first fracturing the

adjacent softer layer. Tentative calculations[7] indicate that by selecting equal thicknesses of soft and hard alloys and by using a fairly strong (150 Ksi = 1 GN/m^2) soft layer, the design aims can be closely approximated.

In the Phase II tensile properties study, the model alloy complex contained a common commercial tool steel (hard layer) and a special alloy (soft-layer). The hard layer (O1 tool steel quenched and tempered to 200°C) had a medium-high hardness of 780 KHN and exhibited no ductility. The specially designed soft layer (Section 2.3.1) Purdue S2 had a hardness of 400 KHN and exhibited about 5% tensile elongation (Figure 6). A preoxidation step was included in fabricating the complex so that interlayer welding would be imperfect. A study of the effect of oxidation time on the tensile properties of the complex showed that an oxidation time of 2 hours in air at 600°C sufficies to increase ductility at little sacrifice of strength. This treatment was incorporated in the fabrication process for complexes with soft layer fracture varying from 0 to 1. For this series of alloy complexes the tensile properties behaved as predicted from the theory referred to above, i.e., the strength varied according to the law of mixtures and appreciable ductility was absent until the fraction soft layer exceeded 0.5. This is expected because the crack jumping mechanism[7] is not favored above this fraction soft layer. The best properties produced at fs = 0.5 were not impressive but are encouraging, 270 Ksi (1.9 GN/m^2) and 3% plastic strain. The fracture behavior was also interesting. Extensive debonding and necking of individual soft layers occurred during fracture raising hopes for significant fracture toughness. In general the Phase II experimental program bore out the theoretical strategy previously described[7] and provides a more solid foundation for designing a higher strength alloy complex.

Future work includes measurement of interlayer bonding to complete Phase II and then the development, testing, and evaluation of the Phase III

alloy complex. Work on these areas is progressing satisfactorily. The bond-test method is already developed (Sections 2.5 and 3.1). The hard layer for the Phase III alloy complex has been tentatively selected as a commercial high-speed steel with a very fine grain size and high hardness. A compatible soft layer is to be designed and a vender has been tentatively located to produce it in sufficient quantities for a significant mechanical properties measurement program including fracture toughness. This alloy will be designed to approach the target strength and toughness.

REFERENCES

1. Lange, E. A., Metals Engineering Quarterly, 11 (1971) 31-39.

2. Zackay, V. F., J. Iron and Steel Inst., 207 (1969) 896-901.

3. Gergerich, W. W., Hemings, P. L., Zackay, V. F. and Parker, E. R., Fracture (1969), Ed , Pratt, P. L., Chapmen Hall, Lond.

4. Winchell, P. G. and Chen, Y. C., ARPA Renewal Proposal (Nov. 1973).

5. Gilman, J. J., J. of Appl. Phys., 31, (1960) 2208-2218.

6. Harrison, H., Vacuum Melter (In preparation for publication).

7. Winchell, P. G. and Chen, Y. C., ARPA Semi-annual Technical Report (Dec. 1973).

8. Krauss, G. and Cohen, M., Trans. of Met. Soc. of AIME, 224, (1962) 1212-1221.